

Role of Glycosylation of IL-1ra on its Binding to IL-1R1

By

Kevin Michael Hutchison

Submitted to the graduate degree program in Pharmaceutical Chemistry and the Graduate Faculty of the University of Kansas in partial fulfillment of the requirements for the degree of Master of Science.

Chairperson Thomas Tolbert

Teruna Siahaan

Zhuo (Michael) Wang

Date Defended: September 3rd, 2015

The Thesis Committee for Kevin Hutchison
certifies that this is the approved version of the following thesis:

Role of Glycosylation of IL-1ra on its Binding to IL-1R1

Chairperson Thomas Tolbert

Date approved: September 4th, 2015

Abstract

Interleukin 1 (IL-1) is an inflammatory cytokine that helps the immune system fight disease. The inflammatory action of IL-1 is regulated by the naturally occurring interleukin 1 receptor antagonist (IL-1ra). IL-1ra contains one N-linked glycosylation site and is expressed in humans in both glycosylated and non-glycosylated forms. The one current IL-1ra drug available (Kineret®) is expressed in *Escherichia coli* as a non-glycosylated form. Because of this, most studies of IL-1ra have been done with the non-glycosylated form and the effects of glycosylation have not been studied. This research attempts to study the effects of the glycosylation of IL-1ra with its binding to the interleukin 1 receptor type 1 (IL-1R1). Both IL-1R1 and IL-1ra were expressed in a glycosylation deficient strain of *Pichia pastoris*. In-vitro binding experiments between the two proteins were studied using both biolayer interferometry and size exclusion chromatography. Due to the long dissociation rate between IL-1ra and IL-1R1, biolayer interferometry was an unfeasible method. Size exclusion chromatography, however, proved to be a promising tool to study binding. Initial experiments with non-glycosylated IL-1ra showed a potential K_D of 1.7 nM. Future studies need to be done using the glycosylated form of IL-1ra to determine any differences in binding between the glycosylated form and the non-glycosylated form.

Acknowledgements

I would like to thank the Department of Pharmaceutical Chemistry at the University of Kansas for the support of this research. I would like to express my gratitude towards my advisor Dr. Thomas Tolbert for his supervision, knowledge, and advice with my research and to my committee members Dr. Michael Zhuo Wang and Dr. Teruna Siahaan for reviewing this thesis. I would like to also thank members of the Tolbert laboratory whose help proved invaluable - Khalid Al-Kinani, Dr. Shaofeng Duan, Solomon Okbazghi, Ishan Shah, and Derek White. I would further like to thank the following: Derek White for expressing the sortase enzyme, expressing IL-1ra in *E. coli*, and ligating fluorescein onto IL-1ra; Dr. Shaofeng Duan for synthesizing the biotin and 5(6) carboxyfluorescein probes used in sortase mediated ligation; and Ishan Shah for performing mass spectrometry on my samples.

Table of Contents

Introduction and Background	1
Introduction.....	1
Background.....	1
Interleukin 1 (IL-1)	1
Interleukin 1 receptor type 1 (IL-1R1).....	2
Interleukin 1 receptor antagonist (IL-1ra).....	3
IL-1 associated inflammatory diseases	4
IL-1ra based drugs	4
Previous IL-1R1 binding studies and methods	5
Conclusion	6
Experimental.....	6
Materials and Methods.....	6
Production of expression plasmid for IL-1R1 containing a C-terminal sortase/histidine tag	7
Expression of IL-1R1 containing a C-terminal sortase/histidine tag	9
Secondary purification of IL-1R1 by hydrophobic interaction chromatography.....	10
Expression of IL-1ra	10
Sortase Reactions	11
Sortase mediated ligation of biotin to IL-1R1.....	11
Sortase mediated ligation of fluorescein to IL-1R1	11
Sortase mediated ligation of fluorescein to IL-1ra.....	11
Binding studies of IL-1ra to IL-1R1 using biolayer interferometry	12
Binding studies of IL-1ra to IL-1R1 using size exclusion	13
Results and Discussion	14
Expression of IL-1R1	14
Expression of IL-1ra	17
Sortase mediated reactions.....	18
IL-1R1 sortase mediated ligation of biotin	18
Sortase mediated ligation of fluorescein to IL-1ra and IL-1R1.	19
Binding experiments of IL-1ra to IL-1R1 using biolayer interferometry	19
Binding studies of IL-1R1 to IL-1ra using size exclusion chromatography	22
Future work.....	25

Figures	27
Reaction Schemes	46
References.....	48
Appendencies.....	50

Introduction and Background

Introduction

Interleukin 1 (IL-1) signaling is inhibited by the competitive binding of the interleukin 1 receptor antagonist (IL-1ra) to the interleukin 1 receptor (IL-1R). IL-1 is an inflammatory cytokine that helps the immune system fight off disease.¹ IL-1 plays a role in both the innate and adaptive immune system. IL-1 can induce an inflammatory signal leading to inflammation, fever and immune cell recruitment. It can induce T cell proliferation so it also has a role in the adaptive immune system.² High levels of the IL-1 or low levels of IL-1ra can lead to autoinflammatory disease. In humans, IL-1ra is produced in both a glycosylated form and a non-glycosylated form. A non-glycosylated IL-1ra drug (Kineret®) has been developed to help regulate IL-1 signaling. Various binding studies of IL-1ra to IL-1R1 have been done in cell based assays - an in vitro cell based assay,³ a competition assay using IL-1 β , IL-1 α , or IL-1ra with IL-1R1 and IL-1R2,⁴ a competition assay between IL-1 α or IL-1 β and IL-1ra for binding to IL-1R1,⁵ and cell proliferation assays.⁶ Studies of the effect of glycosylation on the binding between IL-1ra and IL-1R1 have not been attempted. The objective of this thesis is to determine the effect of glycosylation on the binding between IL-1R1 and IL-1ra.

Background

Interleukin 1 (IL-1)

IL-1 is a cytokine about 17.5 kDa in size and consists of two main forms, IL-1 α and IL-1 β .⁷ IL-1 β is not secreted in the mature form from monocytes. It is synthesized in the cytosol when associated with cytoskeletal structures and remains in the cytosol as an active precursor. When the cell dies it is released and the precursor can be cleaved by extracellular proteases. IL-1 α is usually found in circulation during severe disease. IL-1 β differs in that it is not active as a

precursor and becomes active after cleavage by a protease and is then secreted. When the cell encounters an endotoxin such as LPS, transcription of pro-IL-1 occurs.¹ Before secretion, pro-IL-1 is cleaved by an intracellular cysteine protease (caspase-1) to form the mature form of IL-1. Monocytes constitutively produce caspase-1 while macrophages require a stimulus to produce it.⁸ After cleavage IL-1 is passively secreted from the cell and can bind with IL-1R1 throughout the body. Both of these forms bind to the interleukin 1 receptor (IL-1R). In the body there are two forms of receptor, interleukin 1 receptor type 1 (IL-1R1) and interleukin 1 receptor type 2 (IL-1R2) that can bind IL-1, IL-1, or IL-1ra.

Interleukin 1 receptor type 1 (IL-1R1)

IL-1R1 is an 80 kDa receptor with an extracellular 40 kDa region. When IL-1 binds to IL-1R1 it forms a heterotrimeric complex with the interleukin-1 receptor accessory protein (IL-1RAcP).⁹ This complex promotes a signaling cascade leading to the activation of nuclear factor- κ B (NF- κ B), c-Jun N-terminal kinases (JNKs), and p38 mitogen-activated protein kinase pathways.¹⁰ These induce the expression of other proinflammatory proteins such as IL-6 and IL-8.¹⁰ These events lead to an inflammatory signal recruiting immune cells and causes fever and vasodilation to help fight infection. Endothelial cells are induced by the IL-1 signal and produce adhesion molecules on their surface allowing recruitment of immune cells.¹¹ Cell surfaces can be densely populated with IL-1R1 receptors; however, IL-1 only needs to bind to a few receptors on the surface to initiate an inflammatory response.² So small changes in the amount of IL-1 in the body can lead to disease.

IL-1R1 is heavily glycosylated with six potential glycosylation sites. It was shown that removing the glycans from IL-1R1 leads to a reduction in binding affinity of IL-1 to IL-1R1.

The same researchers showed that glycosylation of IL-1R1 was required for proper transport to the cell membrane.¹²

IL-1R2 is able to bind both IL-1 α and IL-1 β but lacks a cytoplasmic domain and does not produce an inflammatory signal. For this reason, IL-1R2 is thought to be a decoy receptor sequestering IL-1 so it is unable to bind to IL-1R1.¹

Because of the amount of cell receptors and the small amount of IL-1 that is needed to produce an inflammatory signal, regulation of IL-1 is important. Other than regulation by IL-1R2, an important form of regulation comes from a naturally occurring antagonist (IL-1ra).

Interleukin 1 receptor antagonist (IL-1ra)

IL-1 binding is regulated by a naturally occurring interleukin 1 receptor antagonist (IL-1ra). Human IL-1ra has a naturally occurring N-linked glycosylation site and is produced as a mixture of glycosylated and non-glycosylated forms; however, the type of glycosylation is unknown.⁵ The reason that the body produces both forms of IL-1ra is unknown. It is believed that the glycosylation of IL-1ra does not affect the ability of IL-1ra to inhibit IL-1 inflammatory response. However, it is also believed that glycosylation of IL-1ra might protect the protein from degradation in the extracellular space.¹³ The glycosylated form of IL-1ra is approximately 19 kDa while the non-glycosylated form is approximately 17 kDa.

Regulation occurs because when IL-1ra binds, it creates a conformational change that does not allow binding of the accessory protein and subsequent signaling. IL-1ra has been shown to bind to all three domains of IL-1R1 while IL-1 has been shown to bind to only two, leading to the change in conformation.^{9, 14} It has also been shown that while both IL-1ra and IL-1 have similar binding affinities (205 pM for IL-1 β /IL-1 α versus 115 -140 pM for IL-1ra using in vitro cell based assays)³; a 10 to 100 fold excess of IL-1ra is required to inhibit IL-1.² This

inhibition is due to cells having a large number of receptors on the surface. Since only a few receptors are required to initiate an inflammatory response, IL-1ra must be bound in excess to the surface receptors to inhibit the inflammation signal.²

IL-1 associated inflammatory diseases

While IL-1 signaling is important in helping the body fight infection, high levels of IL-1 or low levels of IL-1ra have been linked to many diseases. One of the more noted diseases is rheumatoid arthritis. In rheumatoid arthritis a high level of IL-1 in the synovial fluid leads to an attack of collagen and inflammation in the joints. This attack of collagen damages the bone. IL-1ra drugs were created to help regulate IL-1 signaling.¹⁵

Cryopyrin-associated periodic syndromes (CAPS) are a class of diseases that cause periodic fever syndromes due to mutations resulting in constitutive activation of caspase-1 and excessive secretion of IL-1.¹¹ These diseases include Muckle-Wells syndrome, familial cold autoinflammatory syndrome (FACS) and neonatal-onset multisystem inflammatory disease (NOMID). FACS symptoms such as a rash, headache, and fever occur after the skin is exposed to cold. Muckle-Wells syndrome leads to rash like lesions without the skin being exposed to cold. NOMID is a disease that causes chronic inflammation resulting in a skin rash present from birth and tissue damage of the nervous system and joints.¹⁶

IL-1ra based drugs

The only IL-1ra drug developed so far has been Kineret® (anakinra) made by the Swedish Orphan Biovitrum (Sobi). Kineret® is a non-glycosylated form of IL-1ra expressed in *E. coli*¹⁵ and is used to treat both rheumatoid arthritis and NOMID. Kineret® is given in 100 mg doses by subcutaneous injection once a day.¹⁵ Studies have shown that systemic inflammation was reduced with anakinra including reduction in joint destruction.¹⁷ The half-life of the drug is

short, around 4-6 hours.¹⁵ Because of the large injection needed and once a day dose, injection site inflammation is common and patient compliance difficult.

Previous IL-1R1 binding studies and methods

Previous binding studies have been done in cell based assays using radiolabeled protein. Dripps et al. did binding studies using ³⁵S-IL-1ra, ¹²⁵I-IL-1 and murine thymoma cell line EL4.IL-2 cells at 4°C. Cell bound IL-1ra was measured and a Scatchard plot was created to determine binding. This research gave a reported K_D of 205 pM for IL-1 and 115-140 pM for IL-1ra.³

A competition assay between IL-1ra and IL-1 binding to IL-1R1 was performed by Bienkowski et al.⁵ They used the human monocyte cell line THP-1 to produce IL-1ra and did competition assays by measuring the inhibition of 50 pM ¹²⁵I-IL-1 on YT cells. They found IC₅₀ values from 0.60 to 1.15 nM for IL-1ra displacing IL-1.

A competition assay using surface plasmon resonance (SPR) was created using both IL-1R1 and IL-1R2 from synovial fluids immobilized on a BIAcore chip and introducing varying concentrations of either IL-1ra, IL-1, or IL-1 at room temperature.⁴ It was found that IL-1 bound tighter to IL-1R2 than either IL-1 or IL-1ra and that IL-1ra bound tighter to IL-1R1 than either IL-1 or IL-1.⁴

An inhibition assay was performed by Takii et al.⁶ Various concentration of IL-1ra was used to inhibit 1U/mL of IL-1 induced cell growth of D10N₄M cells at 37°C. These cells were grown for three days in the presence or absence of IL-1ra. They were able to find an IC₅₀ of around 11 nM.

Binding studies using in vitro cell based assays possess some problems. Internalization of the complex could lead to higher binding affinities. Also, interactions with other receptors on the cell surface might lead to altered binding.

Conclusion

IL-1ra is a naturally occurring antagonist produced by the body in both glycosylated and non-glycosylated forms. IL-1ra is able to bind to IL-1R1 and prevent an inflammatory signal. Many IL-1 associated diseases can be treated using non-glycosylated IL-1ra. Binding studies done using in vitro cell based assays have shown a reported K_D of 115-140 pM for IL-1ra. These binding studies present some problems and have not measured the effects of IL-1ra glycosylation. This thesis attempts to develop a binding assay to determine the effects of glycosylation of IL-1ra on the binding to IL-1R1.

Experimental

Materials and Methods

Restriction enzymes (Not I, Xho I, Pme I) were obtained from New England BioLabs®. The plasmid pPICz A, competent Top 10 F' *Escherichia coli*, and *Pichia pastoris* were obtained from Invitrogen™. Yeast nitrogen base was obtained from Sunrise Biosciences. Tryptone and yeast extract were obtained from Becton Dickinson. General chemicals were obtained from Sigma-Aldrich or Fisher Scientific. The nitrocellulose membrane used for the dot blot was a BioTrace™ NT pure nitrocellulose transfer membrane from Pall Corporation. Antibodies used for the dot blot (Pierce™ 6x His epitope tag and Pierce™ Goat Anti-Mouse IgG (H+L), Alkaline Phosphatase conjugated) and 1-Step™ NBT/BCIP used for development were obtained from Thermo Scientific. Protein samples were reduced with 10 mM dithiothreitol (DTT). The protein samples were analyzed using LC/MS. Samples were desalted on a reverse phase C4 column,

50mm, 4.6mm I.D. (Vydac 214MS, 300 Å pore size, 5 µm particle size) using a Agilent 1200 series Liquid Chromatography system. The solvents used were A (99.9% H₂O, 0.08% formic acid, 0.02% TFA) and B (99.9% acetonitrile, 0.08% formic acid, 0.02% TFA). A gradient was developed from 5% B to 90% B in 7 min with a flow rate of 0.5ml/min. They were then analyzed by electrospray ionization mass spectrometry using a Agilent 6520 Quadrupole Time-of-Flight (Q-TOF) system. The instrument was operated in positive ion mode and spectra were acquired covering mass range from 300-3000 m/z with acquisition rate of 1 spectra/second. BioConfirm software Qualitative Analysis (Agilent, Version B.03.01) was used to collect data. Protein MW was calculated using Maximum Entropy Deconvolution function within the software.

Hydrophobic interaction chromatography was done using a GE Healthcare Life Sciences HiPrep™ Phenyl FF HIC column. An 80 mL column was made using SP-Sepharose fast flow resin from GE Healthcare Life Sciences. UV/Vis was done using a Beckman Coulter™ DU® 530 UV/vis Spectrophotometer. Biolayer interferometry was done using a fortéBIO BLItz® system with fortéBIO Dip and Read™ Streptavidin Biosensors and analyzed using BLItz Pro™ Software 1.1. Size exclusion chromatography was done using a 300 x 7.8 mm Yarra 3 µm SEC 3000 and Shimadzu HPLC system.

Production of expression plasmid for IL-1R1 containing a C-terminal sortase/histidine tag

The extracellular domain of IL-1R1 was cloned by conducting PCR using primers (3'-GCCGCGCGCGCGGCCGCTTAATGATGATGGTGGTGGTGGTGCCTCCAGTTTCTGGCAATCCCTTCTGGAAATTAGTGACTGGATATATT -5' and 5'-GGCCCGCTCGAGAAAAGACTGGAGGCTGATAAATGCAAGG-3') and the cDNA for IL-1R1 from the Mammalian Gene Collection (MGC:79368)¹⁸ inserted as a template. The PCR product was restriction digested by Not I and Xho I and ligated into the plasmid pPICz A using

DNA ligase. The pPICz A with the inserted DNA formed the new plasmid pPICz A-IL-1R1-LPETGGG-his6, was transformed into competent Top 10 F' *E. coli* using electroporation,¹⁹ and then selected for on LB-zeocin plates (1% (w/v) tryptone, 0.5% (w/v) yeast extract, 1% (w/v) NaCl, 1.5% (w/v) agar, 25 µg/mL zeocin). The plasmid was purified and the insert was confirmed by DNA sequencing. The plasmid was linearized with *PmeI* and transformed into a competent *P. pastoris* strain with deleted OCH1 using electroporation and selected for using YPD-zeocin plates (2% (w/v) tryptone, 1% (w/v) yeast extract, 2% (w/v) dextrose, 2% (w/v) agar 100 µg/mL zeocin). The plates contained multiple colonies. Ten colonies were picked and screened for higher expression. The colonies were transferred into 2 mL cultures. Once dense, the cultures were induced with methanol (0.5% (v/v) every 12 hours) for 3 days. After three days each culture was screened for IL-1R1 expression by a dot blot.

The dot blot was created by pipetting 5 µL of the induced cultures onto a nitrocellulose membrane. The membrane was allowed to dry and then blocked with 20 mL of TTBS (20 mM Tris-HCl, 500 mM NaCl, 0.05% tween 20) and 5% milk for 1-hour at room temperature (22°C). After 1-hour 5 µL of the primary antibody was added (6x-His Epitope tag) to the blocking solution and allowed to incubate for 6 hours at 4°C. The blocking/antibody solution was removed and the membrane was washed with TTBS. 20 mL TTBS with 5% milk was added to the membrane with 5 µL of the secondary antibody (alkaline phosphatase conjugated anti-mouse IgG (H+L) made in goat) and incubated at 4°C for 6 hours. The blocking/antibody solution was again removed and washed with TTBS and the blot was developed using NBT/BCIP. The blot developed a purple color for the His tagged proteins. A frozen stock was prepared from the highest expressing colony.

Expression of IL-1R1 containing a C-terminal sortase/histidine tag

A 2 mL culture of *P. pastoris* transformed with pPICz A-IL-1R1-LPETGGG-his6 was grown from the frozen stock in YPD media (2% (w/v) tryptone, 1% (w/v) yeast extract, 2% (w/v) dextrose, 100 µg/mL zeocin) at 25°C for 3 days and transferred to a 50 mL flask containing YPD media. This 50 mL culture was grown for 2 days at 25°C and transferred into a 1 L spinner flask containing culture media (1% (w/v) yeast extract, 2% (w/v) tryptone, 1.34% yeast nitrogen base, 2% (w/v) dextrose, 0.1 M potassium phosphate, pH 6.0, 4×10^{-3} % (w/v) histidine, 4×10^{-5} % (w/v) biotin). The 1 L culture was grown at 25°C with air being introduced at 3 L/min. After 3 days the culture was induced with methanol for an additional 3 days (0.7% v/v methanol every 12 hours). The culture was centrifuged at 6,693 G for 20 min and the supernatant was collected. The supernatant was adjusted to a pH of 7.8, refrigerated overnight at 4°C to allow for any precipitate to settle and filtered using Whatman 1 filter paper. After all precipitate was removed, the supernatant was concentrated from 1 L to 200 mL using a Vivaflow 200 10,000 MWCO concentrator. Purification of IL-1R1-LPETGGG-his6 was done using a Ni-NTA agarose column. First the column was equilibrated with equilibration buffer (50 mM potassium phosphate, pH 7.8). Next the concentrated supernatant was loaded and collected. The column was then washed until the absorbance reached baseline using wash buffer (50 mM potassium phosphate, pH 7.8, 500 mM NaCl, 5% glycerol, 20 mM imidazole). Finally the protein was eluted using elution buffer (50 mM potassium phosphate, pH 7.8, 250 mM imidazole). During elution, 6-10 mL fractions were collected by hand based on the UV chromatogram and dialyzed in 20 mM potassium phosphate buffer, pH 7.5, for storage at -20°C. The fractions were checked using SDS-PAGE (Figure 1) to determine which ones contained protein and then confirmed using mass spectrometry (Figure 2). The expected and observed masses are given in Table 1. PNGaseF was used to deglycosylate the protein to check for the full length protein. The protein

concentration was calculated using Beer's Law with an absorbance at 280 nm, path length of 1 cm, and extinction coefficient of $52830 \text{ M}^{-1}\text{cm}^{-1}$. The extinction coefficient was found using the primary amino acid sequence.²⁰ The expression protocol gave a yield of 6 mg/L.

Secondary purification of IL-1R1 by hydrophobic interaction chromatography

The fractions containing protein were pooled together and prepared for hydrophobic interaction chromatography (HIC) by adding solid ammonium sulfate to a final concentration of 1M. About 4 mg of IL-1R1 was loaded onto a 20 mL HiPrep™ Phenyl FF HIC column pre-equilibrated with buffer A (50 mM sodium phosphate, 1 M ammonium sulfate). The protein was eluted with a gradient of 10 column volumes starting with 100% buffer A and finishing with 100% buffer B (50 mM sodium phosphate). 5 mL fractions were collected and checked by SDS-PAGE. The fractions containing protein were pooled together and dialyzed into PBS buffer (50 mM sodium phosphate, 150 mM NaCl, pH 7.4) for binding experiments and stored at -20°C . 1.8 mg of protein was obtained after HIC purification for a yield of 44% for this purification step.

Expression of IL-1ra

Human IL-1ra was previously cloned into pIL-z A and transformed into *P. pastoris* SMD1168H.²¹ Glycosylated and non-glycosylated IL-1ra was produced in yeast and purified as described by Hamilton et al.²¹ The purification chromatogram is shown in Figure 3. The fractions were checked for protein by SDS-PAGE (Figure 4a) and confirmed using mass spectrometry (Figure 4b). The expected and observed masses are given by Table 2. After confirmation, the fractions containing glycosylated IL-1ra were pooled together and the fractions containing non-glycosylated IL-1ra were pooled together. The concentrations were determined by Beer's Law using the extinction coefficient for IL-1ra of $15470 \text{ M}^{-1}\text{cm}^{-1}$ calculated from the primary amino acid sequence.²⁰

Sortase Reactions

Sortase mediated ligation of biotin to IL-1R1

The sortase enzyme was expressed previously by a lab member and used to ligate GGG-EDA-biotin made by another lab member (**Reaction Scheme 1, compound 2**) to IL-1R1-LPETGGG-his6 (**Reaction Scheme 1, compound 1**). IL-1R1 was prepared for sortase ligation by dialyzing the protein in sortase buffer (50 mM tris, 150 mM NaCl, pH 7.5). A 1.5 mL sortase reaction was performed using 3 μ M sortase, 3 μ M IL-1R1, 2 mM CaCl₂, 1 mM GGG-EDA-biotin. The reaction scheme is provided in **Reaction Scheme 1** with the completed reaction yielding IL-1R1-biotin (**Reaction Scheme 1, compound 3**). The reaction was incubated at 37°C for 24 hours and quenched with 10 mM EDTA.²² Completion of the reaction was checked using mass spectrometry (Figure 5). The expected and observed masses are shown in Table 3. The yield was 51% based on the peak intensity found in the mass spectrum. Following confirmation of the completed reaction the reaction was dialyzed in PBS buffer for storage and future binding studies.

Sortase mediated ligation of fluorescein to IL-1R1

IL-1R1 with a sortase tag (**Reaction Scheme 2, compound 1**) was dialyzed into sortase buffer for sortase ligation. A 500 μ L reaction was performed (2.5 μ M sortase, 2.5 μ M IL-1R1, 1 mM GGG-EDA-5(6) carboxyfluorescein (**Reaction Scheme 2, compound 2**) made by a lab member, 2 mM CaCl₂). The reaction scheme is provided in **Reaction Scheme 2** with the completed reaction yielding IL-1R1-FL (**Reaction Scheme 2, compound 3**). The reaction was incubated at 37°C for 24 hours then quenched with 10 mM EDTA.

Sortase mediated ligation of fluorescein to IL-1ra

A lab member ligated fluorescein to IL-1ra in a 3 mL reaction. **Reaction Scheme 3** shows the reaction of IL-1ra with a sortase tag (**Reaction Scheme 3, compound 1**) being ligated

to GGG-EDA-fluorescein (**Reaction Scheme 3, compound 2**) yielding IL-1ra-FL (**Reaction Scheme 3, compound 3**). After the ligation, the product was purified using a Ni-NTA agarose column. To remove sortase and excess fluorescein the reaction was dialyzed after confirmation from mass spectrometry (Figure 6). The reaction gave a yield of 88% fluorescently labeled protein from analysis of the peak intensities from the mass spectrum. Table 4 shows the expected and observed masses.

During the course of purification and dialysis the protein becomes more dilute and could have some loss. Because of this potential change in IL-1ra concentration, the concentration had to be recalculated. The dye can contribute to the absorbance at 280 nm so the concentration of the dye has to be adjusted for when calculating the concentration of IL-1ra according to the following equation:²³

$$A_{\text{protein}} = A_{280} - A_{\text{max}}(\text{CF})$$
$$A_{\text{protein}} = A_{280} - A_{494}(0.30)$$

A correction factor for fluorescein was found by Life Technologies to be 0.30 for fluorescein and the maximum wavelength for absorbance for fluorescein is 494 nm.²³ Using this equation, the absorbance at 280 nm and 494 nm was found and the absorbance of the protein was calculated. After calculating protein absorbance, Beer's Law can be used to find the concentration of the protein, with an extinction coefficient for IL-1ra of 15470 M⁻¹cm⁻¹ calculated from the primary amino acid sequence.²⁰

Binding studies of IL-1ra to IL-1R1 using biolayer interferometry

Biotin labeled IL-1R1 and both glycosylated and non-glycosylated IL-1ra were dialyzed into PBS buffer. The biolayer interferometry (BLI) binding experiment was performed using a fortéBIO BLItz® system with fortéBIO Dip and Read™ Streptavidin Biosensors and analyzed using BLItz Pro™ Software 1.1. The biosensors were hydrated with binding buffer (PBS buffer,

1 mg/mL BSA) for 30 minutes. BSA was used to block any non-specific binding interactions with the biosensor. The biotin labeled IL-1R1 was loaded onto the tip until a loading level of 0.5 nm was achieved. The tips were washed using PBS containing 1 mg/mL BSA. After the tips were washed the binding experiment was carried out. First, a 30-second baseline using binding buffer was done. Then glycosylated IL-1ra at various concentrations (500, 250, 125, 62, 31, 15 nM) was loaded for an association time of 5 minutes. Finally, a 30-minute dissociation was done using binding buffer. A 30-minute dissociation time was decided after increasing the dissociation times due to the observed slow kinetics of dissociation. Two experiments were carried out to test for dissociation over longer times. One experiment used a dissociation time of 2 hours and a second experiment used a dissociation time of 8 hours.

Binding studies of IL-1ra to IL-1R1 using size exclusion

Size exclusion experiments were carried out using a 300 x 7.8 mm Yarra 3 um SEC 3000 and Shimadzu HPLC with a flow rate of 1 mL/min of PBS buffer for 25 minutes. Between each run the loading tip was washed with water for 15 seconds. The column could separate proteins between 244 Da and 670,000 Da. Experiments were done using either the fluorescently labeled IL-1ra (IL-1ra-FL) or IL-1R1 (IL-1R1-FL). Experiments using IL-1R1-FL were done using 500 nM IL-1ra and 3 μ M IL-1R1-FL. These experiments were not continued due to inadequate resolution between the complex and IL-1R1-FL. Experiments using IL-1ra-FL were carried out by keeping the IL-1ra constant (500 pM) while adding various concentrations of IL-1R1 (5000, 2500, 1250, 625, 312.5, 156.25, 78.125 pM). While these concentrations were higher than the reported K_D ,³ these concentrations were chosen because it produced a sufficient fluorescent signal that could be used to track the binding of IL-1ra over the course of the experiment.

IL-1ra-FL and IL-1R1 were both dialyzed into PBS buffer. IL-1ra-FL was diluted from the concentrated stock to 1 nM. IL-1R1 was diluted initially from concentrated stock to 10000 pM and then serially diluted to the final concentrations. The two protein solutions were mixed in a 1:1 ratio and the final concentration of each protein was reached. The solutions were incubated at room temperature (22°C) for 5 hours before injecting 50 µL onto the size exclusion column. A single size exclusion experiment for one sample lasted 25 minutes. Between each experiment the loading tip was rinsed with water for 15 seconds. The protein was detected using a fluorescence detector with an excitation wavelength of 494 nm and an emission wavelength of 521 nm. The peak areas for both the unbound IL-1ra and bound IL-1ra were calculated. A binding curve was created using the percent of bound IL-1ra versus the concentration of receptor. Some experimental issues arose that will be discussed further in the Results and Discussion chapter. The issues were associated with loss of fluorescent signal over the course of the complete experiment.

Results and Discussion

Expression of IL-1R1

The extracellular region of IL-1R1 (MGC: 79368)¹⁸ was cloned with a C-terminal sortase tag and polyhistidine tag (IL-1R1-ST-HIS6) (**Reaction Scheme 1, compound 1**) and subcloned into pPICz A. This region was expressed because it was soluble and needed for binding. The pPICz A vector allowed for expression of the IL-1R1 construct under control of the methanol-inducible Alcohol Oxidase 1 promoter. Additionally, the construct was cloned in frame of the α -mating factor from *Saccharomyces cerevisiae*, allowing for secretion of the construct. A Kex2 site between the α -factor and the IL-1R1 construct allowed for cleavage of the α -factor from the polypeptide.²⁴ The construct was confirmed by DNA sequencing and then transformed into *P.*

Pastoris. IL-1R1 contained both the sortase cleavage site LPETGGG and six C-terminal histidines. The sortase recognition site was added so the IL-1R1 could be ligated with other tags for experiments. In the case of the experiments done in this report, both biotin and fluorescein were added to the C-terminus to be used in the BLItz and size exclusion experiments. The polyhistidine tag allows for purification of IL-1R1 using Ni-NTA agarose chromatography resin. Higher expressing colonies were screened for with a dot blot from 2 mL cultures. The highest expressing colony was selected based on the intensity of the purple color of the blot. After purification the concentration and purity of the protein can be determined. The expression of IL-1R1 was done in a glycosylation deficient strain of *P. pastoris* and yielded an average of 6 mg/L. The glycosylation deficient strain allowed for the production of glycoproteins with high mannose glycans ranging from Man₈GlcNAc₂ to Man₂₀GlcNAc₂.

As can be seen in Figure 1a the purity of IL-1R1 from purification by Ni-NTA agarose chromatography is not high. The SDS-PAGE shows broad bands at around 34 kDa in Lane 1 and around 45 kDa in Lane 2 with smaller, less intense bands indicating impurities throughout the gel. These impurities could be proteolyzed IL-1R1 or other proteins produced by *P. pastoris* that were bound to the Ni-NTA resin. Lane 3 contains glycosylated IL-1R1 while Lane 2 shows non-glycosylated IL-1R1. PNGase F was used to remove N-linked glycans from IL-1R1 to simplify analysis of the protein by SDS-PAGE and mass spectrometry. This will decrease the molecular weight from approximately 45,000 Da for fully glycosylated (6 sites occupied) IL-1R1 to 38186 Da for non-glycosylated IL-1R1. PNGase F can be seen on Lane 2 as a faint band around 35 kDa located between the two darker bands around 40 kDa and 30 kDa. The two darker bands show up in both the glycosylated IL-1R1 lane and the lane containing PNGase F treated IL-1R1. This leads to the idea that the lower band is proteolyzed IL-1R1. IL-1R1 needs

to be pure for binding experiments. Any impurities could affect the calculated concentration of IL-1R1 leading to false binding curves. For BLI the concentration of IL-1R1 is as not important as will be discussed in the section containing binding studies using BLI. However, when doing binding studies using size exclusion, the concentration of IL-1R1 is important.

Because of the impurities seen in Figure 1a, a second purification step was performed. Hydrophobic interaction chromatography (HIC) using a HiPrep™ Phenyl FF HIC column was performed as this second purification step. Fractions from the HIC purification were checked using SDS-PAGE to determine purity and then pooled together. The HIC purification diluted the samples to 0.02 mg/mL for a yield of 1.8 mg or 44%. Because the sample was dilute, the sample was concentrated 10 fold to look for any impurities (Figure 1b). Figure 1b shows, when compared to Figure 1a, that the impurities were removed by HIC. There appear to be no shadows above or below the main band.

Table 1 shows the expected and observed masses found in the mass spectrum located in Figure 2. To determine if the full length protein was expressed and no proteolysis has occurred, the protein was observed using mass spectrometry. For this step the protein was reacted with PNGaseF, an enzyme that cleaves N-linked glycans. During this reaction asparagine is converted to aspartic acid, increasing the mass by 1 Da. In the case of IL-1R1 the expected deglycosylated mass is 38186 Da. If all potential glycosylation sites were occupied, then after deglycosylation the expected mass would be 38192 Da. However, the peak shown in Figure 2a is 38189 Da indicating removal of 3 glycans. Figure 2b shows IL-1R1 with glycosylation.

Figure 2b and Table 1 show that four to six sites are occupied. The glycosylation deficient strain of yeast used gives high mannose glycans. The masses found in Figure 2b shows that 3, 4, 5, and 6 N-linked glycosylation sites are occupied. Each of these sites contains high

mannose glycoforms starting at $\text{Man}_8\text{GlcNAc}_2$ and going to $\text{Man}_{15}\text{GlcNAc}_2$ for some occupied sites. This mass spectrum shows that all 6 glycosylation sites can become occupied during yeast expression; however, when all 6 sites were glycosylated, mannose phosphorylation was observed.

Expression of IL-1ra

IL-1ra was cloned previously by Hamilton et al.²¹ The procedures for the purification of glycosylated IL-1ra using SP-Sepharose and the yeast strain developed in the Hamilton paper were used to express and purify glycosylated and non-glycosylated IL-1ra. These products will be used in future studies when a working IL-1ra binding method has been developed.²¹

Figure 3 shows the UV chromatogram during the purification of IL-1ra using SP-Sepharose as was described by the above purification procedure. As is shown in the figure and as was reported,²¹ the peak for glycosylated IL-1ra can be distinguished from the peak for non-glycosylated IL-1ra. The fractions associated with these peaks were checked on a gel and then the glycosylated IL-1ra was pooled and non-glycosylated IL-1ra was pooled. These were then confirmed using mass spectrometry. As can be seen in the gel (Figure 4a), the purity of both forms of IL-1ra was high so no secondary purification step was needed.

Figure 4b shows the mass spectra for both non-glycosylated IL-1ra and glycosylated IL-1ra while Table 2 shows the observed and expected masses. The table and mass spectrum show that there is one occupied glycosylation site starting at $\text{Man}_8\text{GlcNAc}_2$ up to $\text{Man}_{18}\text{GlcNAc}_2$.

A 1 L yeast expression yielded 5.1 mg of non-glycosylated IL-1ra and 9.9 mg of glycosylated IL-1ra. This amount agrees with the reported expression and purification procedure.²¹

Sortase mediated reactions

Sortase is a cysteine protease that cleaves between threonine and glycine in the sortase recognition site (LPETG) to form a thioester intermediate between the substrate and enzyme. Compounds containing an N-terminal glycine can act as a nucleophile to attack the thioester bond, displacing the sortase enzyme, and forming a peptide bond between the substrate and compound. Sortase mediated ligations are useful because they are site specific, can be used to attach various labels (fluorescein, biotin), only require a C-terminal sortase tag, and the reactions can be carried out under mild conditions (pH 7.5). The activity of the sortase enzyme, however, is limited by the dependence of calcium. The product after ligation is also a substrate for the enzyme that can make it difficult for completion of the reaction.^{22, 25}

IL-1R1 sortase mediated ligation of biotin

IL-1R1 was cloned with a sortase recognition site (LPETG). GGG-EDA-biotin was synthesized by another lab member. After sortase cleavage the GGG-EDA-biotin will ligate to the LPET of the protein shown in **Reaction Scheme 1**. Figure 5 shows the mass spectrum of the product of the sortase mediated ligation of biotin. The biotinylation of IL-1R1 gave us the product IL-1R1-Biotin.

The mass spectrum shows five major peaks. PNGaseF was added to remove the N-linked glycans, however, incomplete glycosylation occurred. Without removal of the glycans the mass spectrum would be too cluttered to properly interpret the success of the reaction. Table 3 shows the expected mass, observed mass, and peak intensities. Using the information in the table, estimation of yield by comparing peak intensities of the product versus the starting material gave a 51% yield.

Sortase mediated ligation of fluorescein to IL-1ra and IL-1R1.

GGG-EDA-5(6)carboxyfluorescein, synthesized by a lab member was ligated to IL-1ra by another lab member. The ligation of fluorescein to IL-1ra gave the product IL-1ra-fluorescein (IL-1ra-FL). In order to remove unreacted IL-1ra the protein was purified by a lab member on a Ni-NTA agarose column. The protein was then dialyzed in PBS buffer to remove unligated fluorescein. Figure 6a shows the difference between purified IL-1ra-FL and the unpurified IL-1ra. As can be seen at the bottom of Lane 1 there remains some unreacted fluorescein which is not present in the purified form in Lane 2. Figure 6 shows the mass spectrum for the ligation of fluorescein to IL-1ra. The reaction was not 100% complete with about an 88% yield based on the peak intensities as shown in Table 4. The final concentration of IL-1ra-FL was 7 μ M.

Fluorescein was also ligated to IL-1R1 and used for initial size exclusion experiments. There was little resolution between the complex and IL-1R1 peaks so further experiments using fluorescently labeled IL-1R1 were not conducted and additional purification was not required.

Binding experiments of IL-1ra to IL-1R1 using biolayer interferometry

BLI allows for the real time kinetic analysis of binding between two molecules. BLI uses a biosensor that is composed of glass fiber containing a bio-compatible layer at the tip. Streptavidin is immobilized on the bio-compatible layer through a proprietary surface chemistry. Streptavidin has a high binding affinity for biotin with a K_D around 10^{-14} M. This allows for immobilization of a biotinylated protein (IL-1R1) for binding studies with a protein in solution (IL-1ra). White light is transmitted through the biosensor and then reflected back. The light is reflected back from two interfaces, one is the bio-compatible layer/glass fiber interface and the other is the solution and surface layer containing the bound protein. The light reflected from these two surfaces will have a different path length. An increase in path length results in constructive or destructive interference between the two reflected light waves leading to an

interference pattern monitored by the instrument and response measured as a shift in nm. A sensor reads the initial interference pattern from the two light waves and can determine a baseline before any addition of the biotinylated receptor. After addition of the receptor the path length increases and a second baseline is recorded. Once this baseline is established IL-1ra can be added. The formation of the IL-1ra/IL-1R1 complex further increases the path length and the interference can be monitored over the course of association. At the end of association, buffer is introduced causing dissociation of complex, decreasing the path length. The kinetic association and dissociation rates are calculated by the instrument based on 1:1 curve fitting and the corresponding association rate constant (k_a), dissociation rate constant (k_d), and dissociation constant (K_D) derived from the ratio of the rate constants can be found.²⁶ Figure 7 shows a general scheme for how a BLI experiment using BLItz should look.

Initial binding experiments were conducted using concentrations of IL-1ra between 500 nM and 15.625 nM. IL-1R1 was loaded to a low level to prevent crowding of the biosensor (Figure 8). These initial experiments were done to determine appropriate receptor loading, association time, dissociation time, and how to remove non-specific binding.

Because non-specific binding occurs between the ligand and the biosensor, 1 mg/mL BSA was added to all samples and buffers. Figure 9 shows how BSA affects both the baseline (with no IL-1R1 added) and the association signal (with IL-1R1 added). With no BSA present IL-1ra binds to streptavidin producing a small association curve. When BSA was introduced as a blocking agent, IL-1ra was unable to bind non-specifically to the biosensor. When the receptor was introduced, addition of BSA had a slight effect on the binding. The association of IL-1ra to IL-1R1 produced a smaller signal than when no BSA was added.

As was discussed previously the IL-1R1 sample was a mixture of biotinylated IL-1R1 and IL-1R1 with a histidine tag. This impurity was not a concern because only the biotinylated IL-1R1 would bind to streptavidin biosensor. Because of this the protein did not undergo any additional purification.

The association times and dissociation times were adjusted based on experiments. The association time was increased to 5 minutes to allow for equilibrium. As can be seen by the binding curves there is little to no dissociation over the course of the experiment. Initially a 2-minute dissociation time was used but the time was increased to 30 minutes due to the slow dissociation. This 30-minute dissociation time was used for an initial attempt at a binding curve as seen in Figures 10a and 10b.

This slow dissociation gave variable K_D 's. The association constants remained relatively close for each run 2.651×10^{-5} to $3.098 \times 10^{-5} \text{ M}^{-1}\text{s}^{-1}$, while the dissociation constants varied considerably between 1.53×10^{-4} and $4.767 \times 10^{-4} \text{ s}^{-1}$ with two samples providing no dissociation at all. Figure 10a shows runs producing negative slopes indicating dissociation, while Figure 10b shows runs producing positive dissociation slopes, indicating something other than dissociation. It is unknown why the positive slopes occur. This increase in signal could be due to the actual dissociation rate being so small that baseline correction errors within the BLItz software could overwhelm the measurement. Because an accurate k_d could not be determined, any determination of K_D was impossible.

Since the dissociation rates measured in different experiments using a 30-minute dissociation time were variable, experiments were done to test how long dissociation might take to occur between IL-1ra and IL-1R1. These experiments used 2-hour and 8-hour dissociation times instead of a 30-minute dissociation time. 8 hours was the maximum time the instrument

collected data. Figure 11a shows the dissociation over 2 hours. As is shown in the figure, no dissociation occurred over that time frame. Figure 11b shows the dissociation over 8 hours. This figure shows an abnormal dissociation curve over the time frame. The curve increases before leveling off and then decreases, which is unexpected for a dissociation curve.

The information gained shows that using BLI to study the binding between IL-1R1 and IL-1ra was impractical because the dissociation rate of the complex was too slow to measure with the BLItz instrument. The slow dissociation of IL-1ra made it difficult to determine the K_D using kinetic measurements. Instead, the K_D was investigated using an equilibrium binding approach.

Binding studies of IL-1R1 to IL-1ra using size exclusion chromatography

The results from the use of BLI showed that the disassociation of IL-1ra is extremely slow. In the experiment shown in Figure 11, even after eight hours there was no noticeable dissociation occurring. Because of this BLI is not suitable for studying this interaction and another binding experiment had to be developed. A method that was thought to be appropriate was size exclusion chromatography. Size exclusion experiments using the Yarra SEC column take about 9 to 11 minutes to elute proteins between 17 kDa and 70 kDa. IL-1ra and the receptor were not expected dissociate within this time frame because no dissociation was detected even after 8 hours using BLI. With the slow dissociation rate between IL-1ra and IL-1R1, the complex would not dissociate over the course of a typical SEC experiment. Size exclusion allows for the resolution between proteins of different sizes. A size exclusion column has pores that trap smaller molecules while the larger ones pass through. IL-1ra is 17 kDa while IL-1R1 is around 45 kDa. When these two proteins bind they form a complex that is around 62 kDa. This size difference was able to be resolved by a Yarra SEC column.

When performing the binding experiment the first step was to determine if IL-1ra or IL-1R1 should be fluorescently labeled. The protein needed to be fluorescently labeled because at the low concentrations used (500 pM) and a 50 μ L injection volume, no protein could be detected at 280 nm. The initial experiments were done before either protein was purified after the sortase ligation so both fluorescently labeled proteins contain unknown impurities that can be seen on the chromatograms.

As is shown in Figure 12a, the peak containing the complex can only be slightly resolved from the peak containing uncomplexed fluorescently labeled IL-1R1. This is expected as the difference in elution times on the Yarra column between the masses IL-1R1 (45 kDa) and the complex (62 kDa) is not that great. This resolution was determined to not be enough to continue doing size exclusion binding using fluorescently labeled IL-1R1. Because of this fluorescently labeled IL-1R1 was not purified any further.

Size exclusion was able to separate the free form of fluorescently labeled IL-1ra from the complex with higher resolution as shown in Figure 12b. Using the information from the two experiments it was determined that using the fluorescently labeled IL-1ra and unlabeled receptor was the best method. The method used was to keep the fluorescently labeled IL-1ra (500 pM) constant while varying the concentration of IL-1R1 (5000, 2500, 1250, 625, 312, 156, 78 pM). Again, while the concentration of IL-1ra is well above the reported K_D of 115-140 pM,³ it was chosen because it produced a good signal that could be used to detect the binding of IL-1ra to IL-1R1 over the course of the experiment. This required additional purification of fluorescently labeled IL-1ra to remove the unknown peaks. After purification of IL-1ra by the method previously mentioned, a binding curve was created.

The samples were incubated at room temperature (22°C) for 5 hours after being mixed together. The concentrations of the components are low so the binding might take a long time to reach equilibrium. A 5-hour incubation time was estimated after results from the BLI experiments (Figure 13) using similar concentrations to what would be used in size exclusion chromatography. Each sample was loaded onto the SEC column 3 times. Between each experiment (25 minutes) is a loss of signal (Figure 14a). This loss was consistent between runs of the same sample (Figure 14b); however, between runs of different samples the peak areas varied. The binding experiment was conducted as described and peak areas were found for both bound IL-1ra-FL and unbound IL-1ra-FL (Figure 15 and appendices). These peak areas were totaled (Table 5). This total peak area varied for different concentrations and was inconsistent. The ratio of bound IL-1ra-FL to unbound IL-1ra between repeat injections, however, was consistent. Because of this, the percentage of IL-1ra-FL that was bound and the percentage that was unbound could be used to create a binding curve (Figure 16). These plots fit expected plots for binding curves.²⁷ As the receptor concentration is increased the percentage bound reaches an equilibrium point. Using the information from these plots, the K_D was found to be 1.7 nM.

Many difficulties were experienced during the experiments using size exclusion chromatography. The first issue was signal loss between runs. This signal loss could be due to adsorption onto the HPLC glass vial inserts. To correct for this, deactivated glass inserts were used. However, the deactivated glass caused even greater peak loss. This loss could be due to an increase in adsorption onto the deactivated glass or the deactivated glass causing a precipitate. Another potential cause of loss could be from adsorption onto the column. When BSA was used it was shown to help prevent signal loss (Figure 17).

Future work

While the method presented proved to be a useful tool to study the binding of IL-1ra to IL-1R1, future work needs to be done to complete the project. The reported K_D for IL-1ra calculated from a cell based assay was 115-140 pM.³ These experiments were conducted at 4°C, which will give a different K_D value than the experiments reported in the thesis at 22°C. The experiments using cell based assays differ from in vitro assays because the complex could become internalized or have interactions with other receptors on the cell surface; however, these assays are closer to how the binding occurs in the body. These cell based assays could help us to develop assays to see how the glycosylation of IL-1ra affects binding in more biologically relevant systems.

The concentration of IL-1ra used for the size exclusion chromatography binding experiment was 500 pM. This concentration is almost 5 times greater than the reported K_D .³ This high concentration could lead to depletion of IL-1R1 leading to an overestimation of K_D . To prevent this, the concentration of IL-1ra needs to be $0.1 \times K_D$ (approximately 10 pM).²⁷ 500 pM was chosen for convenience because it produced a good fluorescent signal that could be used to observe binding. The experiments done in this thesis used an injection volume of 50 μ L. To obtain a good signal while using concentrations of IL-1ra around 10 pM, the injection volume could be increased to an amount that produces an adequate signal, allowing for more accurate binding data.

To reduce peak loss during the size exclusion experiment some changes may prove useful. As was discussed, using BSA as a blocking agent was shown to reduce peak loss. Also, the time duration of the experiment could be decreased. The experiment was conducted over 25 minutes but all components eluted before 15 minutes. Decreasing the experiment time could result in less adsorption to the glass.

An assay to study the binding between glycosylated IL-1ra and IL-1R1 needs to be developed to compare with the results found for the binding between non-glycosylated IL-1ra and IL-1R1. This could be done with a competition assay between the already created non-glycosylated IL-1ra-FL and glycosylated IL-1R1. Another method that could be used would be to add a sortase tag onto the C-terminus of glycosylated IL-1ra and fluorescently label the IL-1ra. After glycosylated IL-1ra is fluorescently labeled, a binding curve could be performed using the same methods already discussed.

Figures

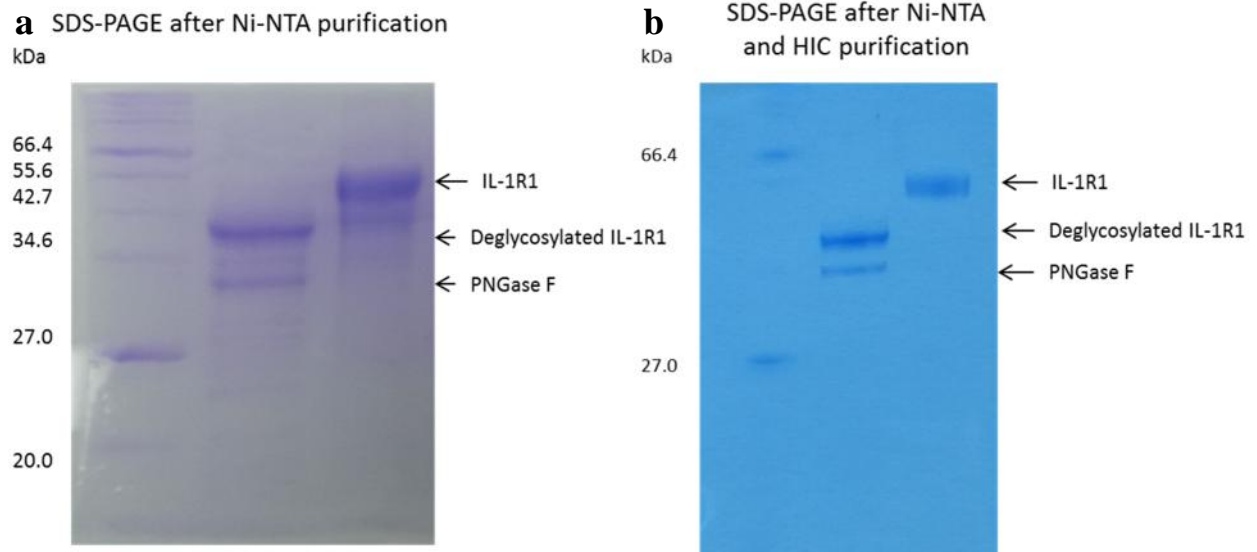


Figure 1: **a)** 12% SDS PAGE showing both glycosylated and nonglycosylated IL-1R1 after Ni/NTA purification. Lane 1: Protein Marker Lane 2: IL-1R1 + PNGase F Lane 3: L-1R1 **b)** 12% SDS PAGE gel of concentrated IL-1R1 after HIC purification Lane 1: marker Lane 2: IL-1R1 Lane 3: IL-1R1 + PNGaseF.

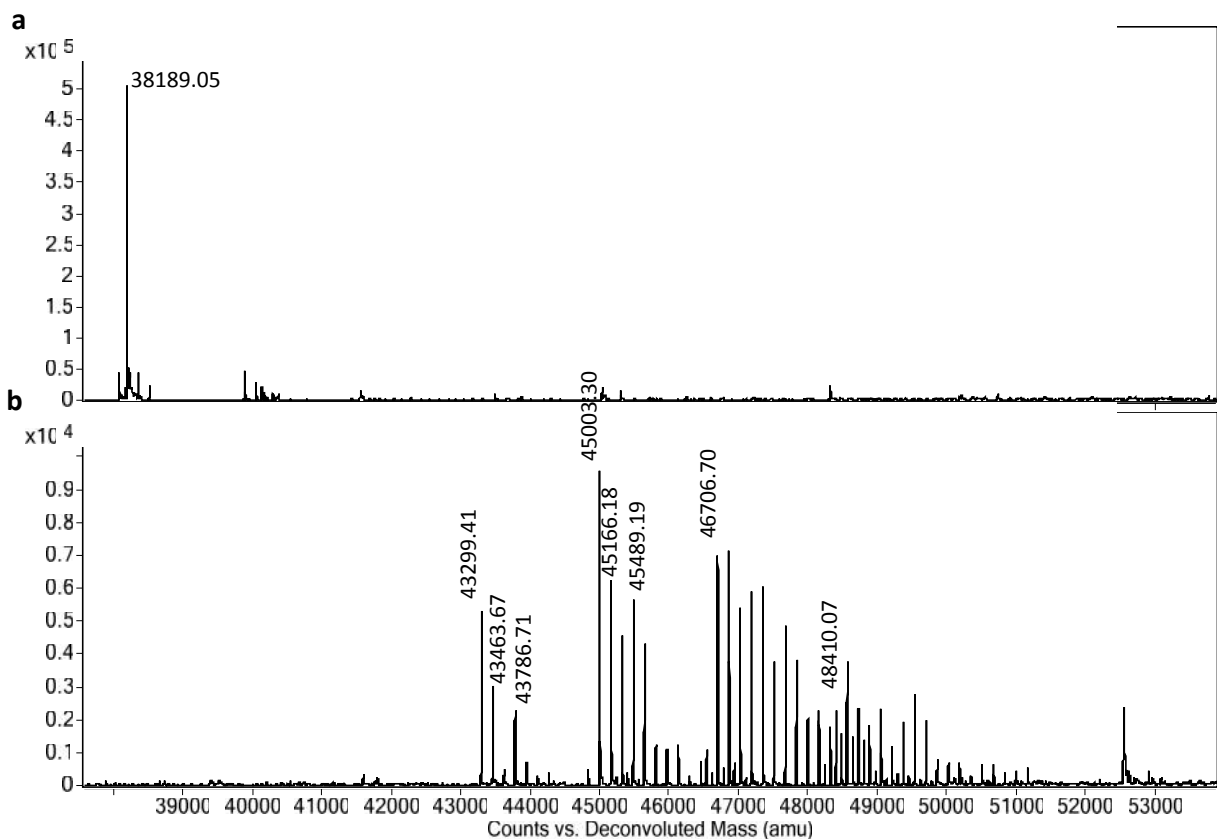


Figure 2: a) Mass spectrum of IL-1R1 treated with PNGaseF. b) Mass spectrum of IL-1R1 showing glycosylation.

Table 1: Table showing expected and observed masses from the mass spectrum from Figure 2.

	Expected Mass (Da)	Observed Mass (Da)
Deglycosylated IL-1R1	38186	38189
3 sites occupied	43293	43299
4 sites occupied	44996	45003
5 sites occupied	46698	46706
6 sites occupied	48401	48410

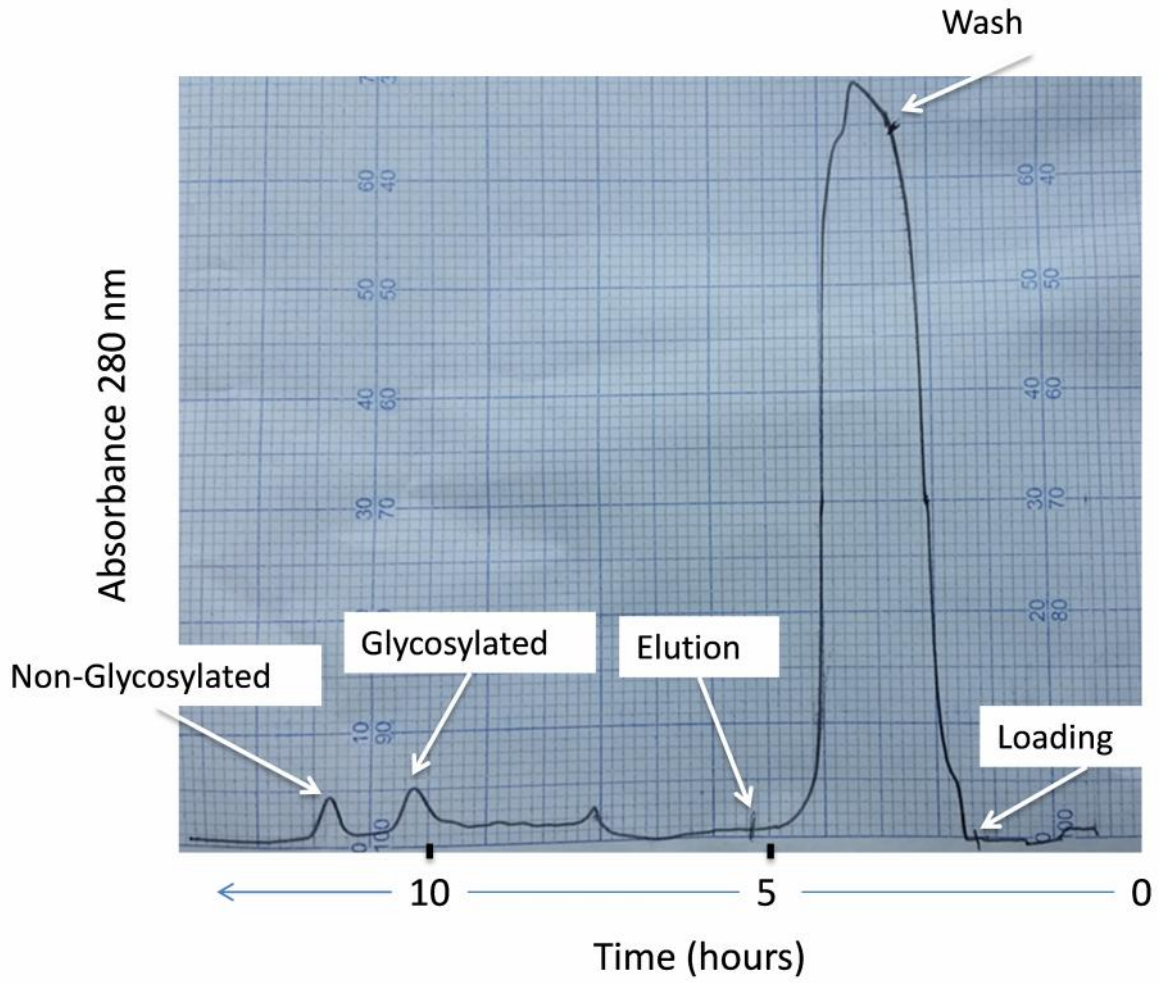


Figure 3: The purification using SP-sepharose was run according to the literature procedure. The UV chromatogram shows the non-glycosylated and glycosylated peaks can be easily resolved.

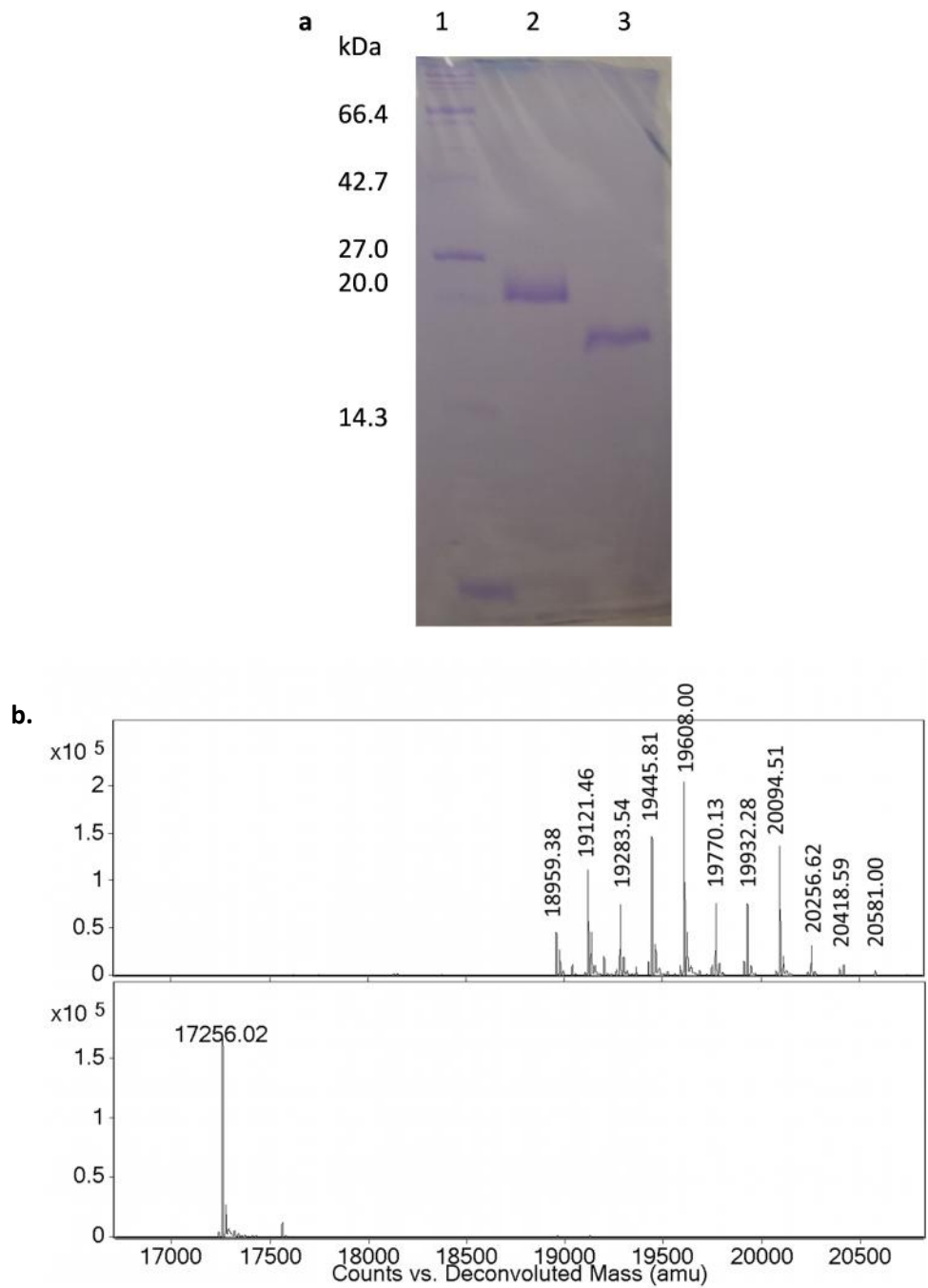


Figure 4: **a)** 12% SDS PAGE of pooled IL-1ra fractions. Lane 1: Marker. Lane 2: Glycosylated IL-1ra. Lane 3: Non-glycosylated IL-1ra. **b)** Mass spectrum for glycosylated IL-1ra (top) showing mannose up to man 18 and mass spectrum for non-glycosylated IL-1ra (bottom).

Table 2: Table showing the expected and observed masses from Figure 4.

	Expected Mass (Da)	Observed Mass (Da)
IL-1ra non-glycosylated	17256	17256
Man₈GlcNAc₂	18958	18959.38
Man₉GlcNAc₂	19120	19121.46
Man₁₀GlcNAc₂	19282	19283.54
Man₁₁GlcNAc₂	19444	19445.81
Man₁₂GlcNAc₂	19606	19608.00
Man₁₃GlcNAc₂	19768	19770.13
Man₁₄GlcNAc₂	19930	19932.28
Man₁₅GlcNAc₂	20092	20094.51
Man₁₆GlcNAc₂	20254	20256.62
Man₁₇GlcNAc₂	20416	20418.59
Man₁₈GlcNAc₂	20578	20581.00

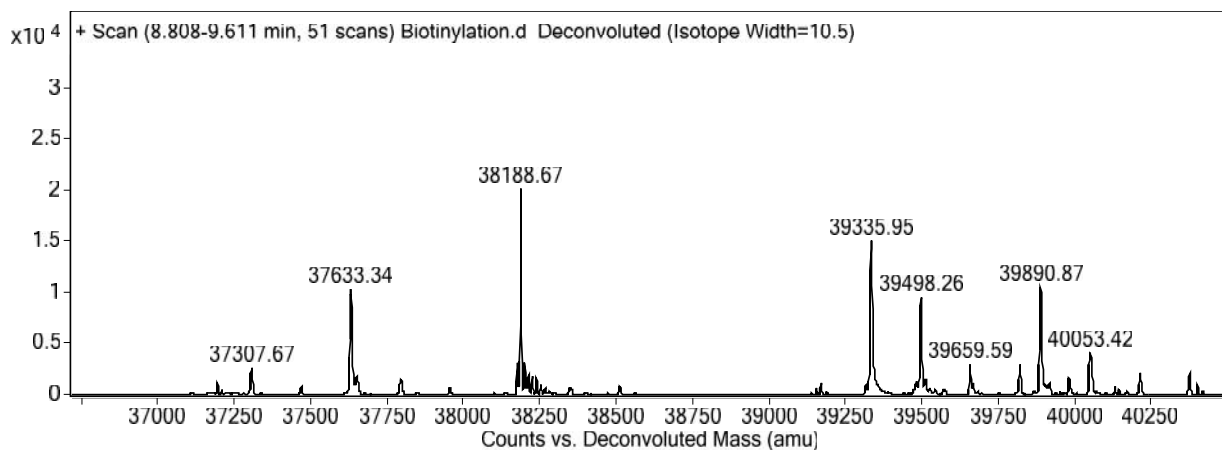


Figure 5: Mass spectrum of the reaction of the biotinylation of IL-1R1.

Table 3: Table showing expected and observed masses for mass spectrum in Figure 5.

	Expected Mass (Da)	Observed Mass (Da)	Peak Intensity ($\times 10^4$)	Percentage
Biotinylated product	37632	37633	1.10	13.3
Biotinylated product + 1 Man₈GlcNAc₂	39334	39335	1.85	22.2
Biotinylated product + 1 Man₉GlcNAc₂	39496	39498	1.25	15.1
Unreacted product	38186	38188	2.20	26.5
Unreacted product + 1 Man₈GlcNAc₂	39888	39890	1.30	15.7
Unreacted product + 1 Man₉GlcNAc₂	40050	40053	0.60	7.2

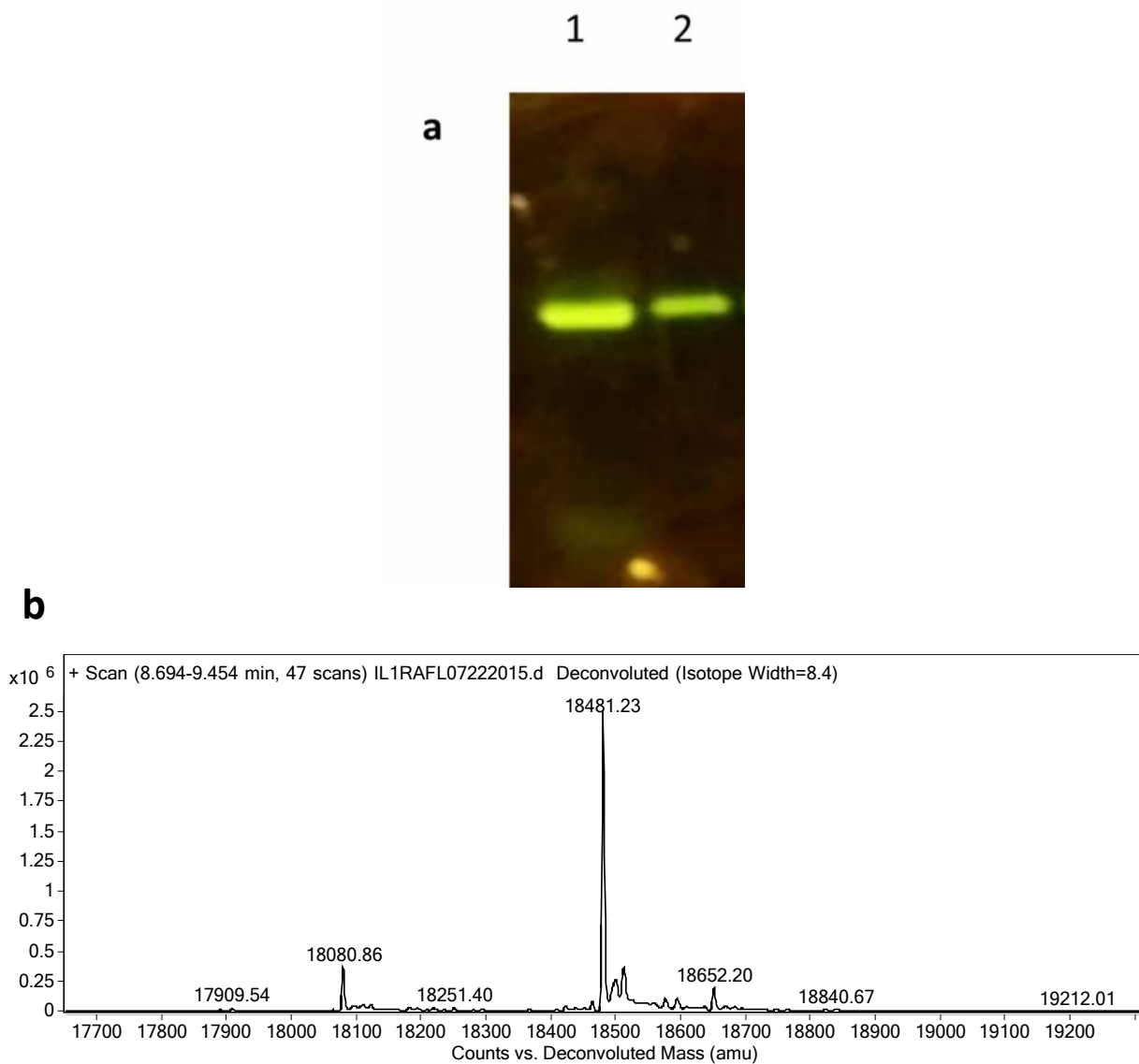


Figure 6: a) 12% SDS PAGE of IL-1ra-Fluorescein. Lane 1: unpurified IL-1ra-Fl. Lane 2: Purified IL-1ra-Fl. b) Mass spectrum of the ligation of 5(6) carboxyfluorescein to IL-1ra.

Table 4: Table showing expected and observed masses for the mass spectrum in Figure 6.

	Expected Mass (Da)	Observed Mass (Da)	Peak Intensity (x10 ⁶)	Percentage
Unligated IL-1ra	18080	18080.86	0.19	12.2
IL-1ra-Fluorescein	18481	18481.23	1.37	87.8

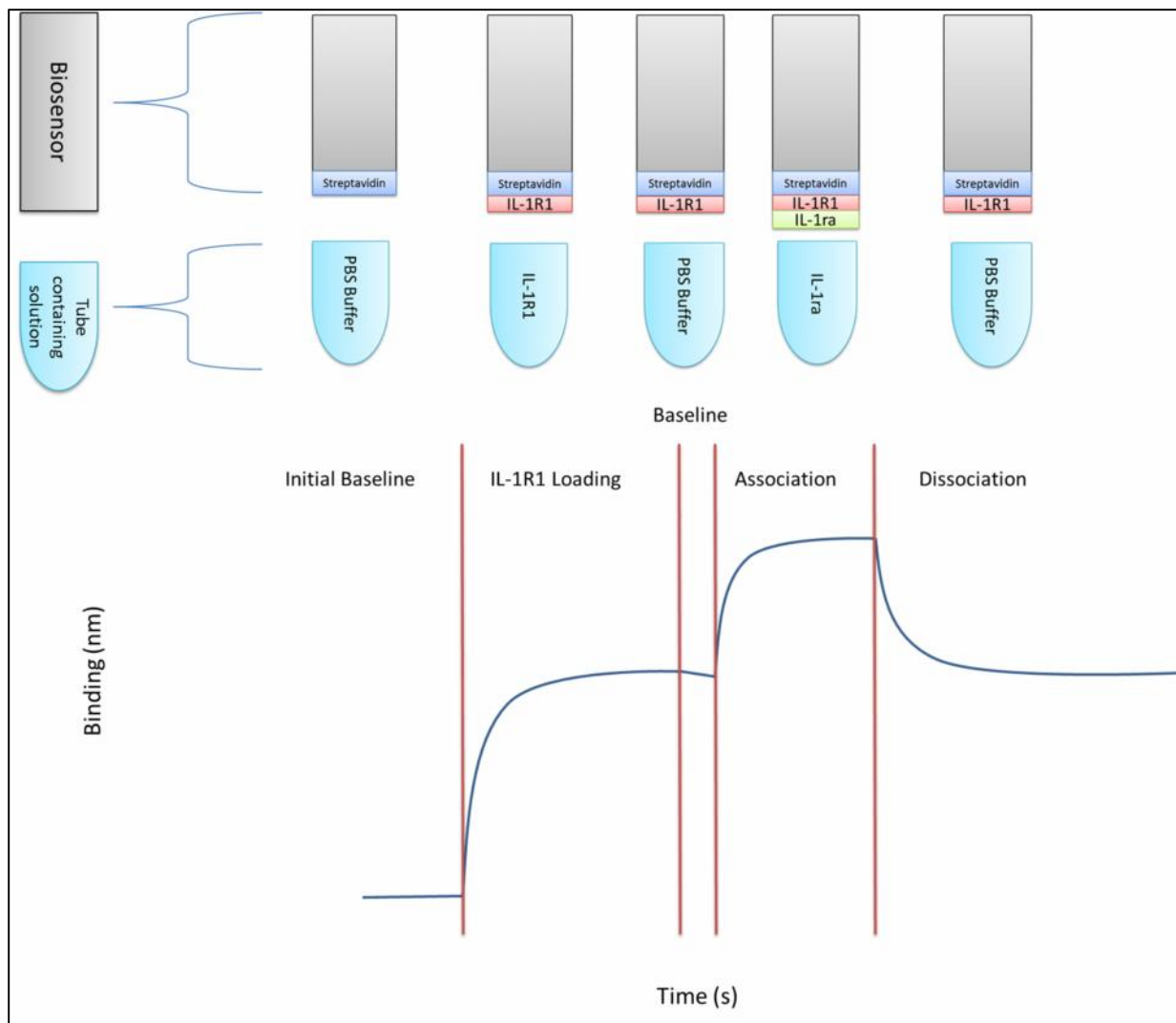


Figure 7: Diagram showing general BLITZ experiment. Step 1: Baseline using PBS buffer, 1 mg/mL BSA. Step 2: IL-1R1 loading. Step 3: Baseline using PBS buffer, 1 mg/mL BSA. Step 4: IL-1ra association. Step 5: Dissociation with PBS buffer, 1 mg/mL BSA.

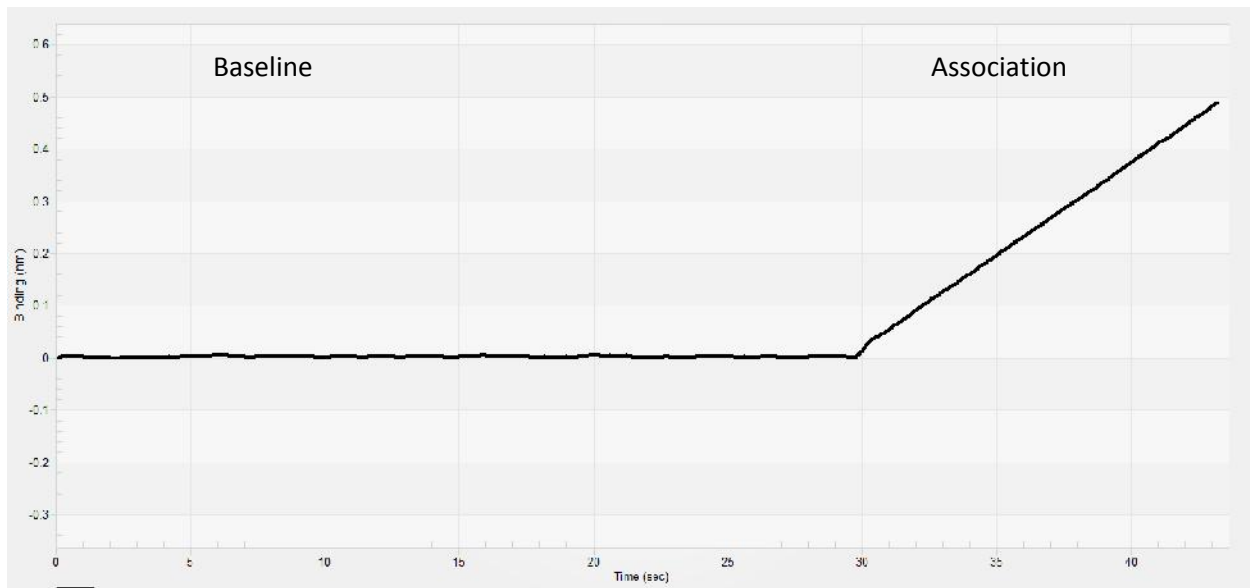


Figure 8: Loading of IL-1R1 to 0.5 nm to prevent crowding of the receptor on the biosensor.

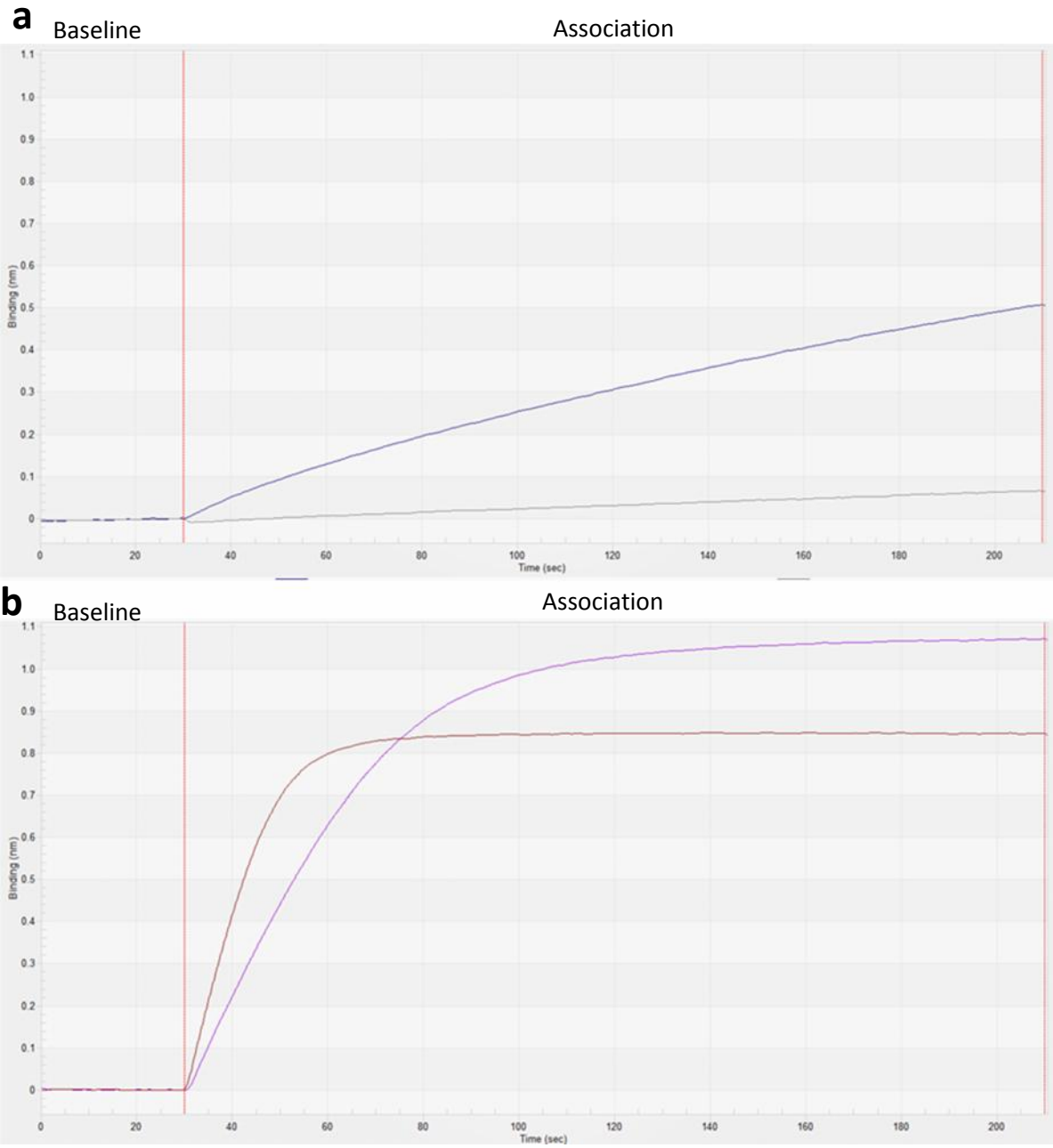


Figure 9: a) nonspecific binding of IL-1ra. Runs contained no IL-1R1 and 0.5 μ M IL-1ra. Grey: Run with 1 mg/mL BSA. Blue: Without BSA. b) Runs contained IL-1R1 and 0.5 μ M IL-1ra. Brown: Runs with 1 mg/mL BSA. Purple: Runs contained no BSA.

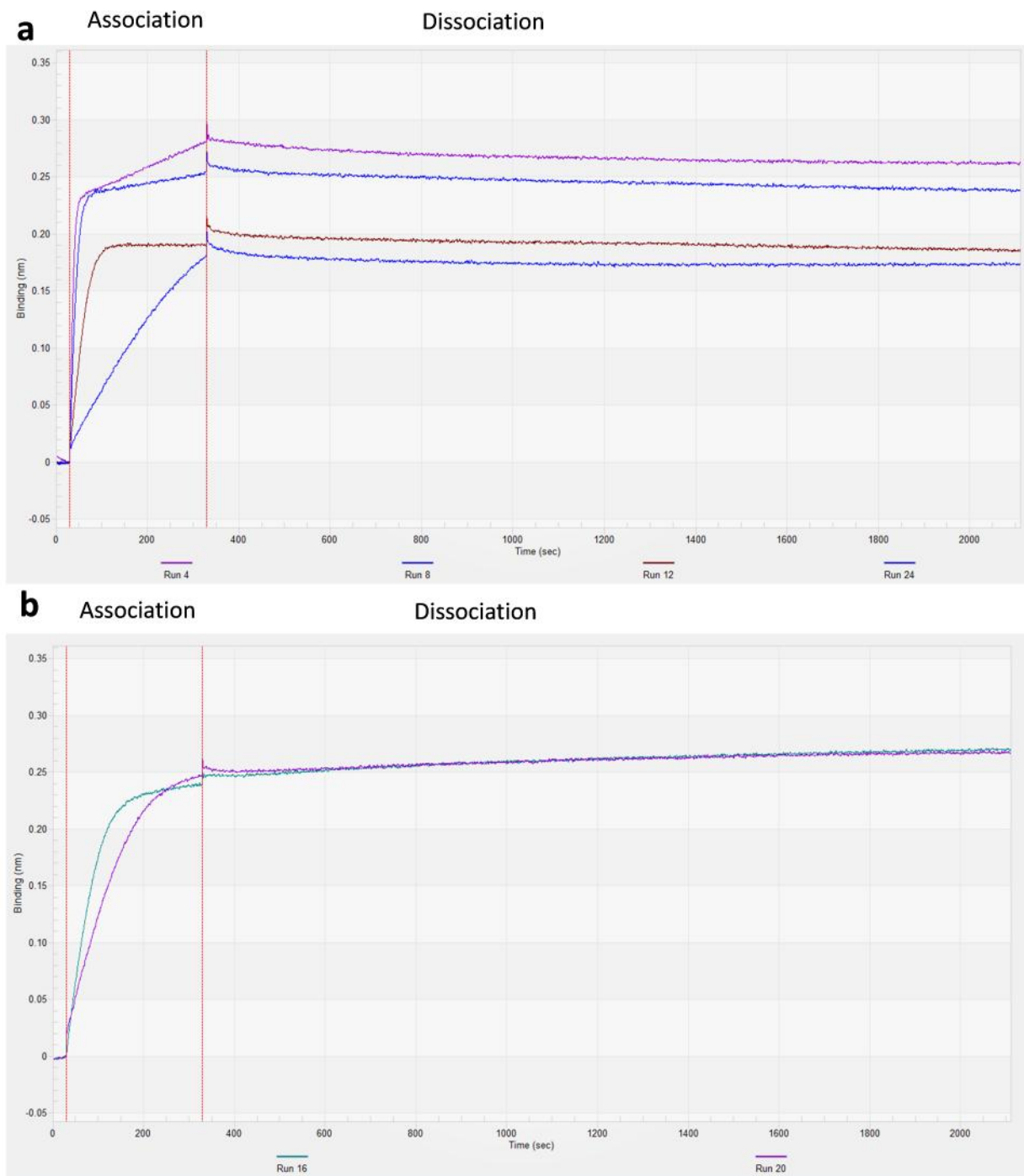


Figure 10: a) BLITZ curves showing binding for runs containing negative dissociation slopes. Run 4: 500 nM. Run 8: 250 nM. Run 12: 125 nM. Run 24: 15 nM. b) BLITZ curve showing binding for runs containing positive dissociation slopes. Run 16: 62 nM. Run 20: 31 nM.

Association

Dissociation

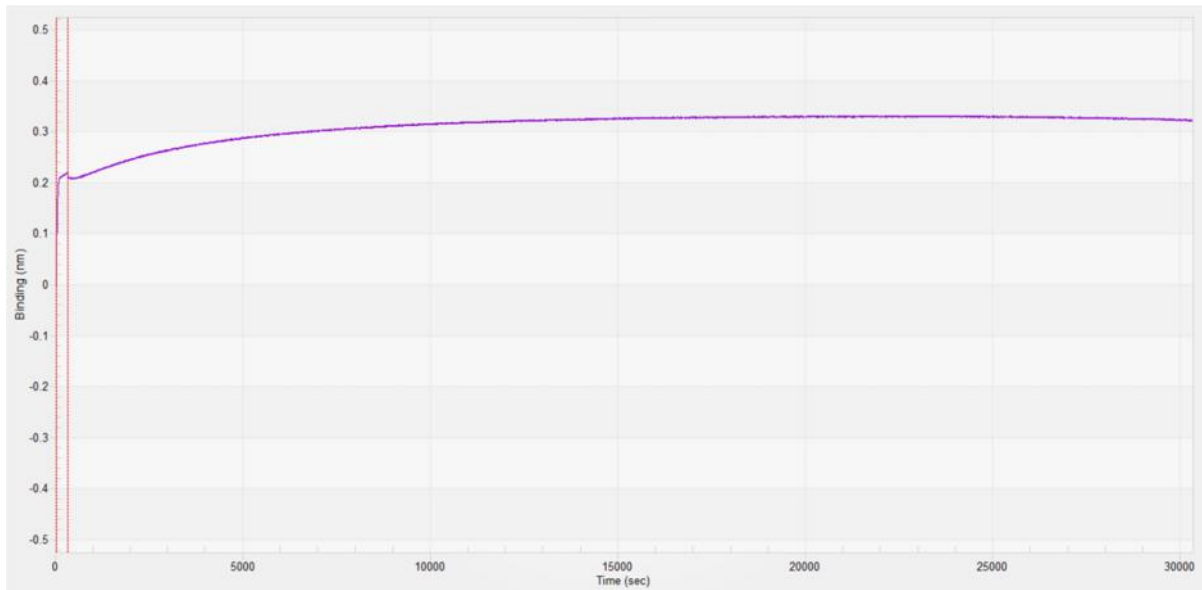
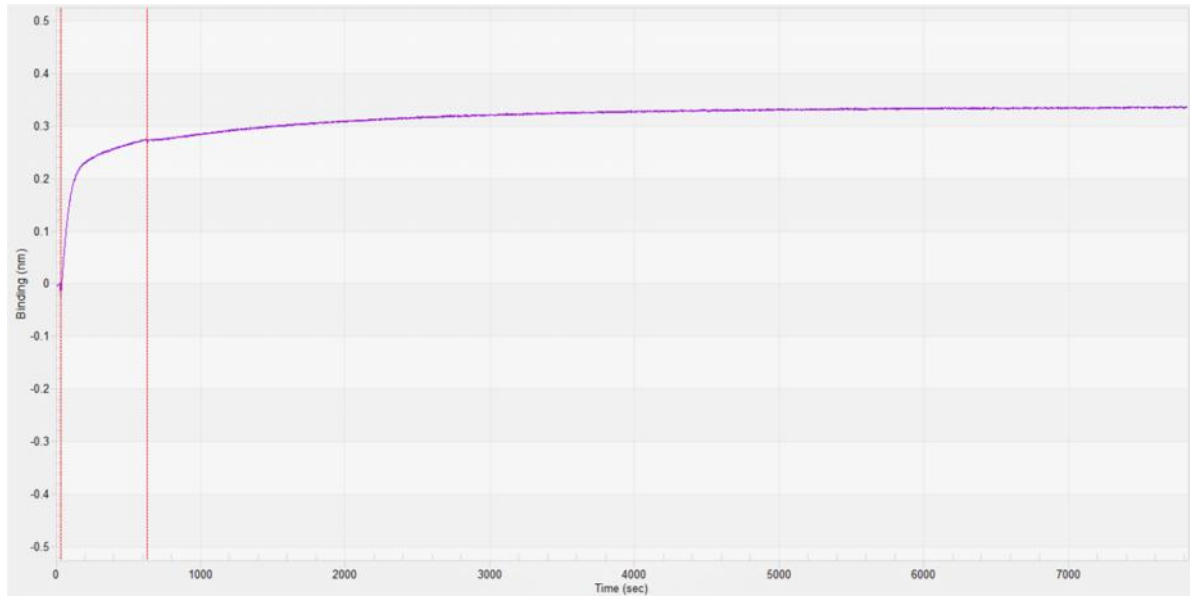


Figure 11: a) 2-hour dissociation curve using BLItz. b) 8-hour dissociation curve using BLItz.

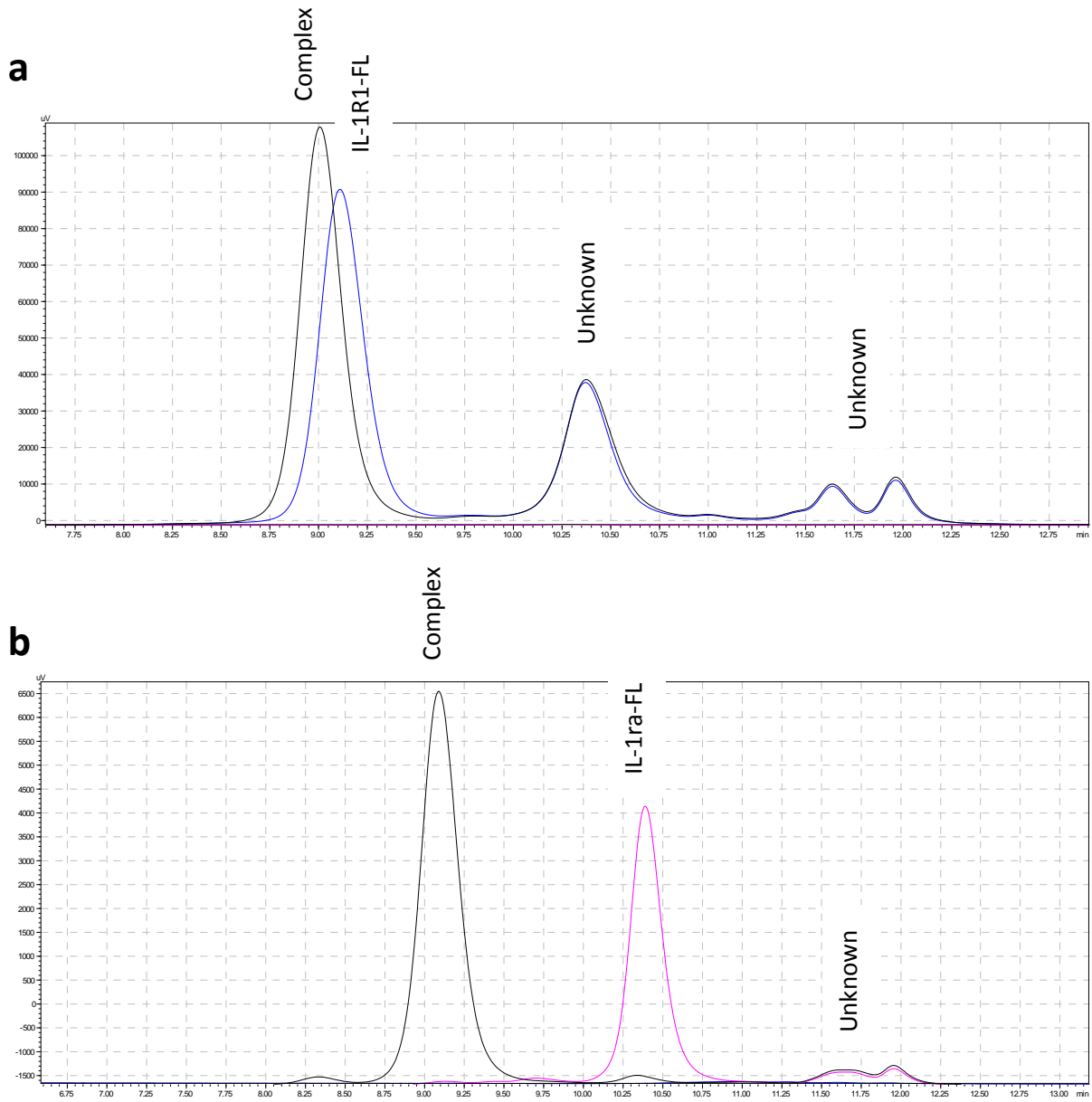
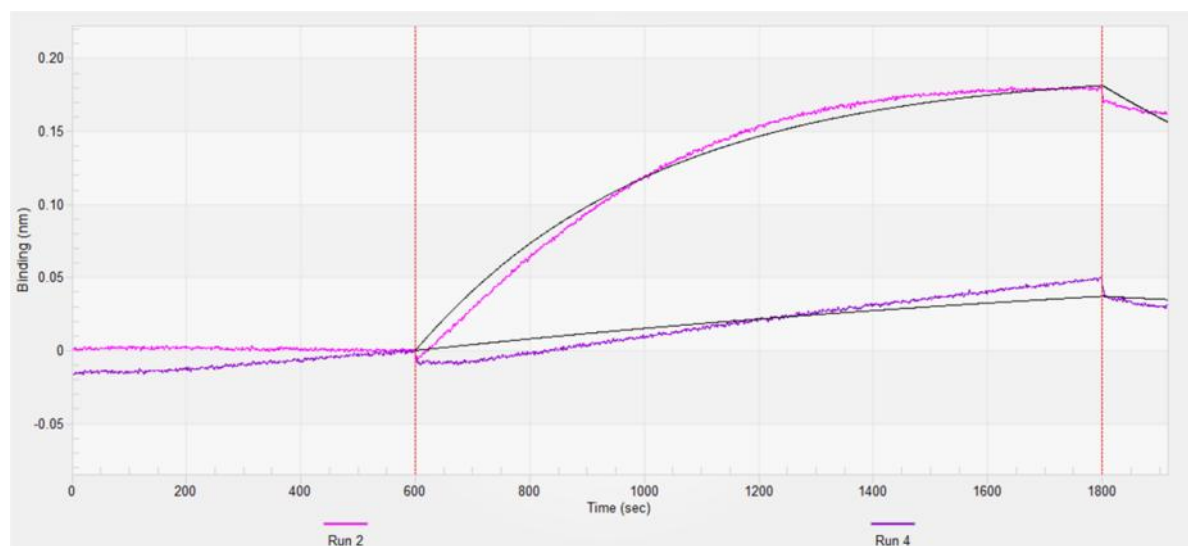


Figure 12: a) 500 nM IL-1ra + 3 μM IL-1R1-FL. Blue line: 500 nM IL-1R1-FL no labeled IL-1ra. Black line: Complex formed between 500 nM unlabeled IL-1ra and 3 μM IL-1R1-FL. b) 500 nM IL-1ra-FL + 3 μM IL-1R1. Pink line: 500 nM IL-1ra-FL and no unlabeled IL-1R1. Black line: complex formed between 500 nM IL-1ra-FL and 3 μM unlabeled IL-1R1.



Run 2: 7.8 nM
ka: 1.563×10^5

Run 4: 0.975 nM
ka: 1.35×10^3

Figure 13: BLItz curve showing runs of low concentration over a 20-minute association time.

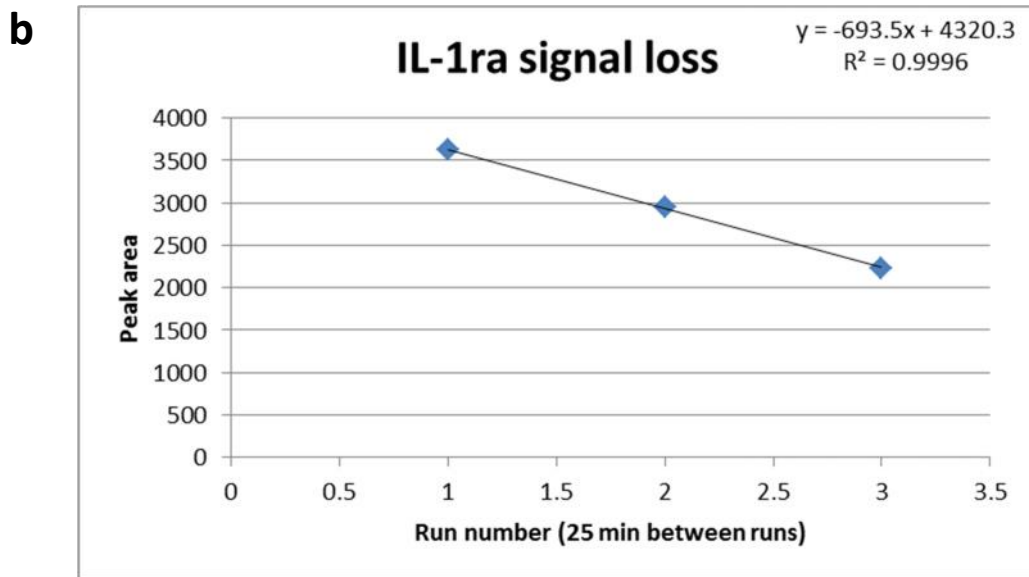
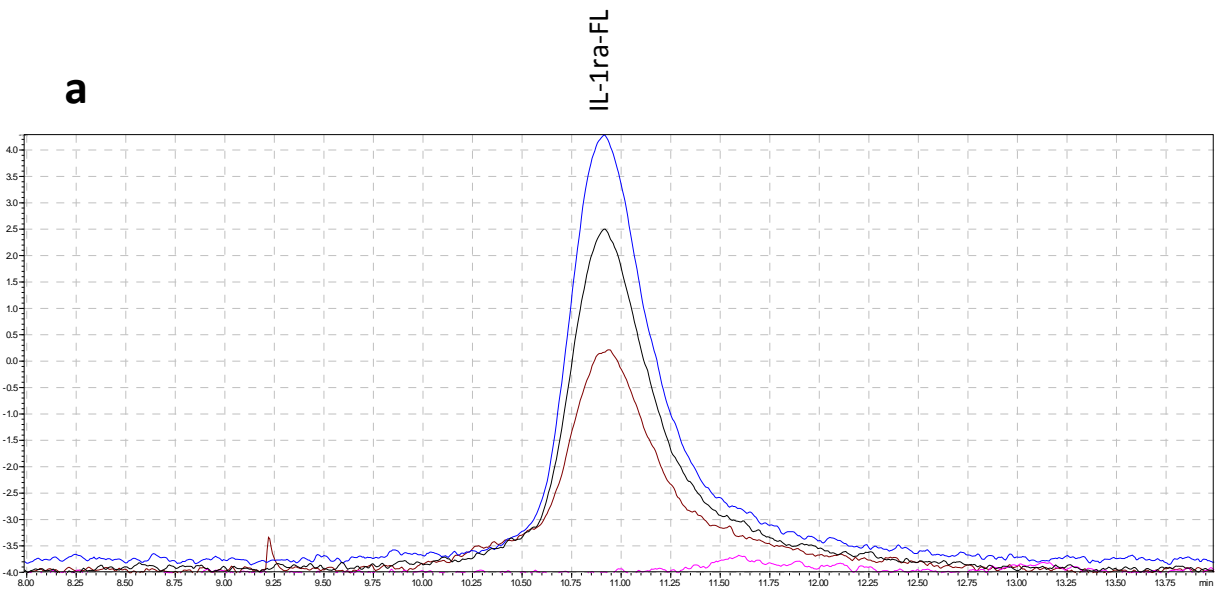


Figure 14: a) 500 pM IL-1ra over 3 runs. Each run is 25 minutes apart. Blue: Run 1. Black: Run 2. Brown: Run 3. b) Chart showing the loss of fluorescent intensity of IL-1ra over the three runs shown in Figure 14a.

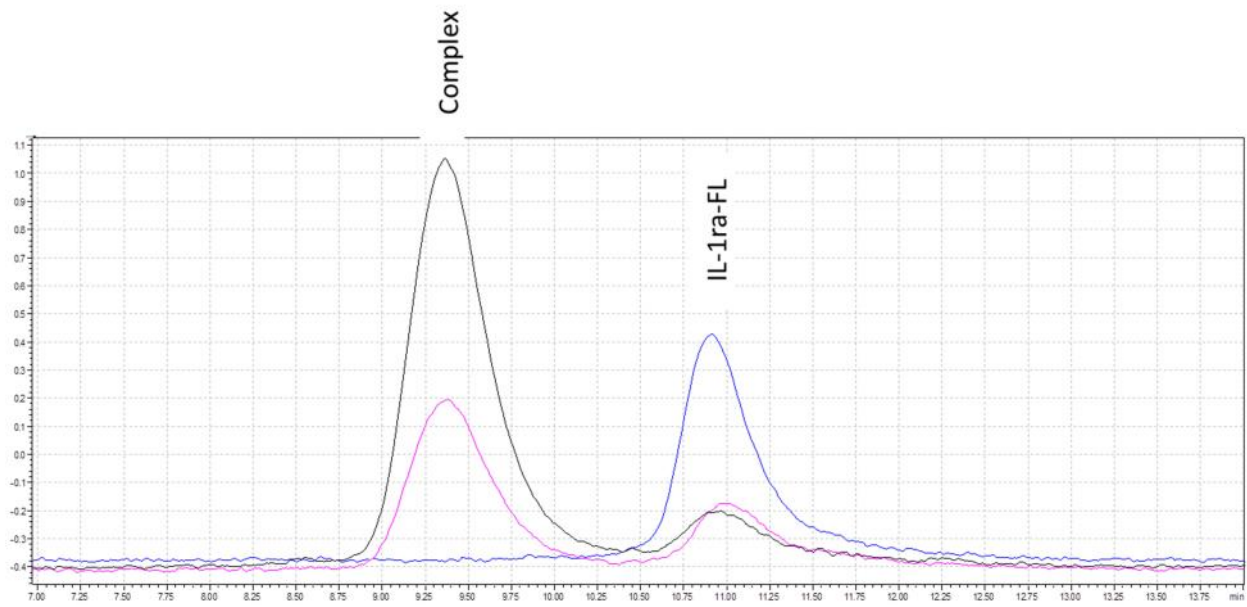


Figure 15: IL-1ra size exclusion run. Blue: 500 pM IL-1ra-FL, no unlabeled IL-1R1. Black: 500 pM IL-1ra-FL, 5,000 pM unlabeled IL-1R1. Pink: 500 pM IL-1ra-FL, 2,500 pM unlabeled IL-1R1.

Table 5: Tables showing the peak area of bound and unbound and the percentage of bound and unbound IL-1ra.

Conc (pM)	Bound	Unbound	Total	%Bound	%Unbound
Run 1					
78	0	1736	1736	0	100
156	58	2598	2656	2.18	97.82
312	108	1699	1807	5.98	94.02
625	574	2060	2634	21.79	78.21
1250	1036	1953	2989	34.66	65.34
2500	1783	399	2182	81.71	18.28
5000	3672	260	3932	93.39	6.61
Run 2					
78	0	1534	1534	0	100
156	49	2305	2354	2.08	97.92
312	108	1182	1290	8.37	91.63
625	488	1713	2201	22.17	77.83
1250	975	1653	2628	37.10	62.90
2500	1486	338	1824	81.47	18.53
5000	3100	178	3278	94.57	5.43
Run 3					
78	0	1349	1349	0	100
156	34	2062	2096	1.62	98.37
312	129	1008	1137	11.34	88.65
625	384	1318	1702	22.56	77.43
1250	886	1670	2556	34.66	65.33
2500	1496	328	1824	82.01	17.98
5000	2650	167	2817	94.07	5.92

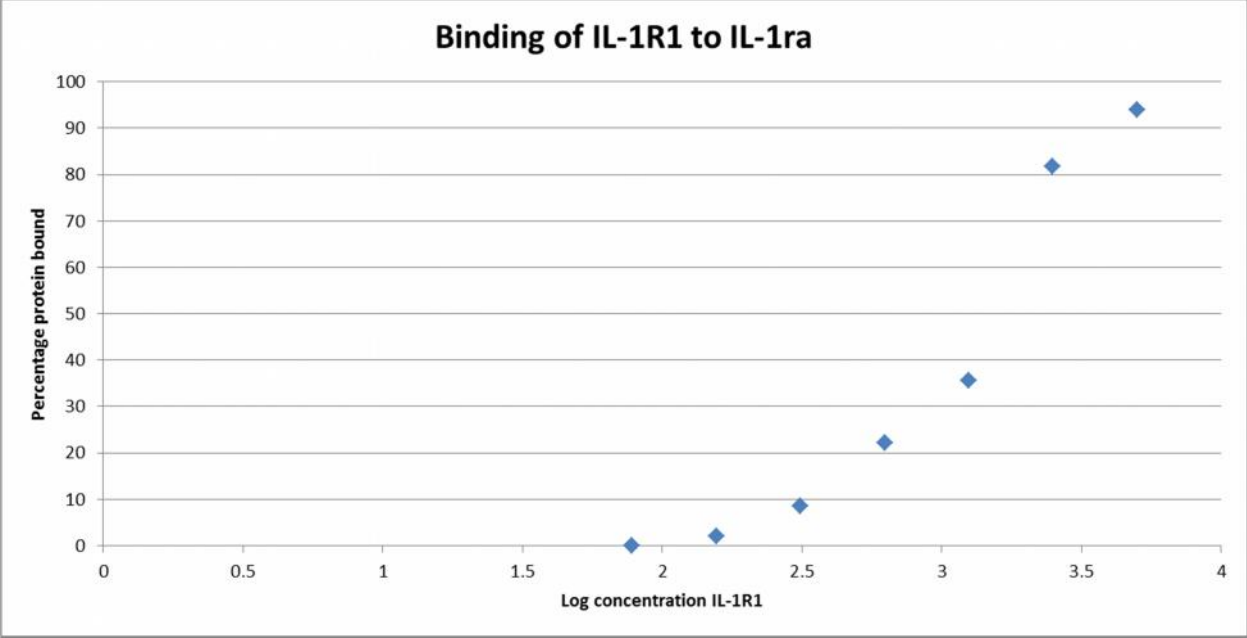
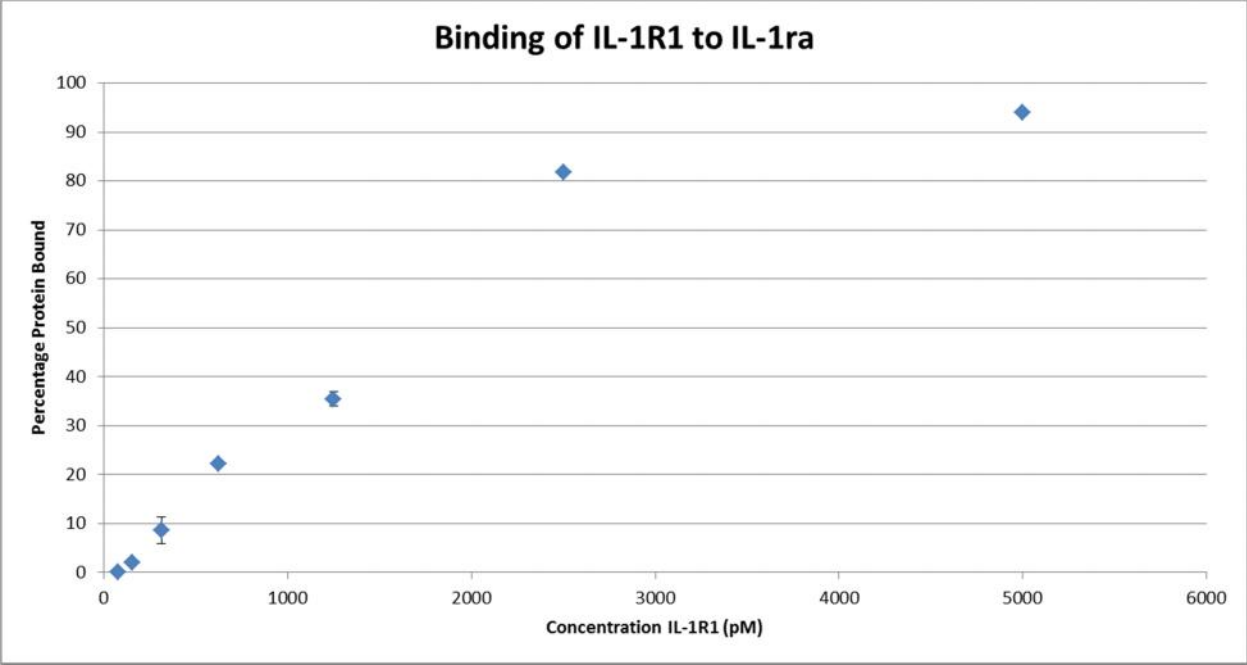


Figure 16: a) Chart showing percentage of protein bound versus the concentration of IL-1R1. b) Chart showing the percentage protein bound versus the log of the concentration of IL-1R1.

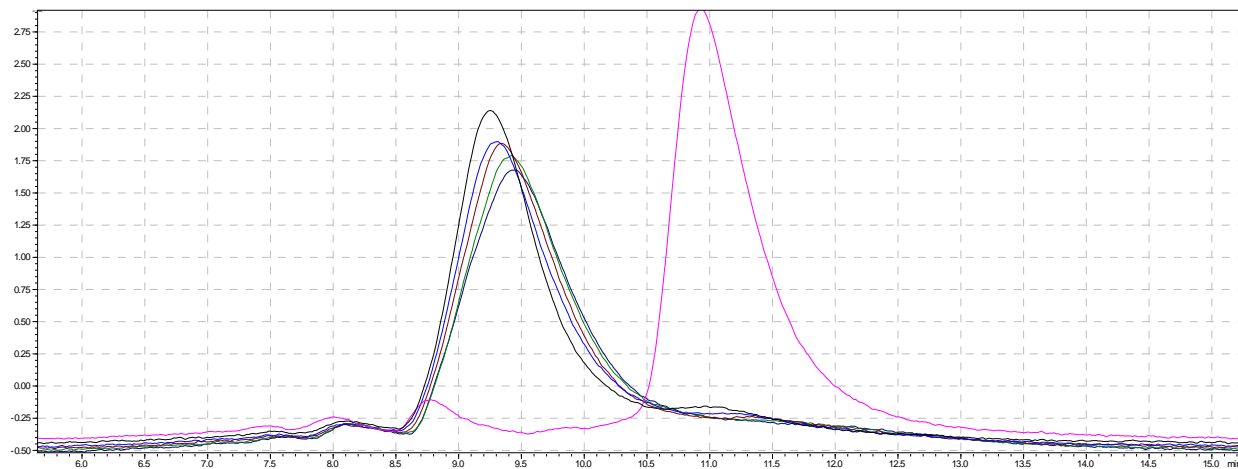
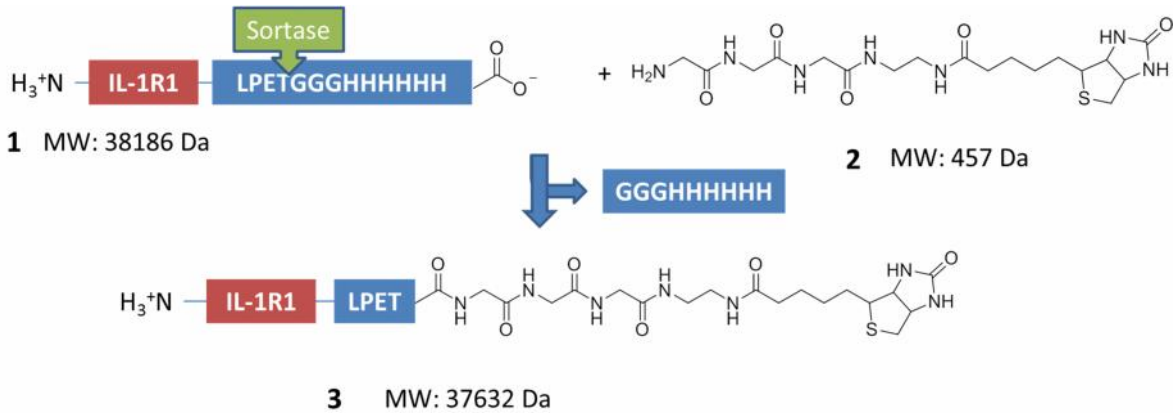
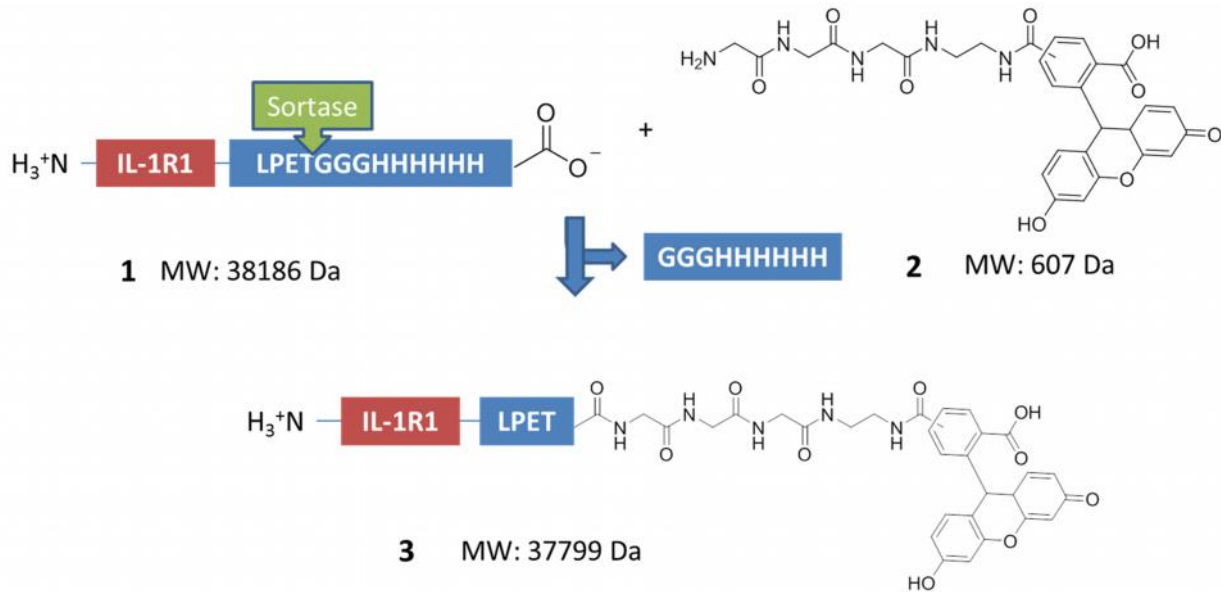


Figure 17: BSA added to complex of 500 pM IL-1ra-FL and 5,000 pM unlabeled IL-1R1.

Reaction Schemes



Reaction Scheme 1: Reaction scheme for the sortase mediated ligation of biotin to IL-1R1. 1) IL-1R1 containing a C-terminal sortase tag and poly histidine tag. 2) Triglycine ethylene diamine biotin. 3) GGG-EDA-biotin ligated to IL-1R1.



Reaction Scheme 2: Reaction scheme for the ligation of 5(6) carboxyfluorescein to IL-1R1. 1) IL-1R1 containing a C-terminal sortase tag and polyhistidine tag. 2) Triglycine ethylenediamine 5(6) carboxyfluorescein. 3) GGG-EDA-fluorescein ligated to IL-1R1.

References

1. Dinarello, C. A., Biologic basis for interleukin-1 in disease. *Blood* **1996**, *87* (6), 2095-147.
2. Arend, W. P., Interleukin-1 Receptor Antagonist. *Advances in immunology* **1993**, *54*, 167-227.
3. Dripps, D. J.; Brandhuber, B. J.; Thompson, R. C.; Eisenberg, S. P., Interleukin-1 (IL-1) receptor antagonist binds to the 80-kDa IL-1 receptor but does not initiate IL-1 signal transduction. *Journal of Biological Chemistry* **1991**, *266* (16), 10331-10336.
4. Arend, W. P.; Malyak, M.; Smith, M. F.; Whisenand, T. D.; Slack, J. L.; Sims, J. E.; Giri, J. G.; Dower, S. K., Binding of IL-1 α , IL-1 β , and IL-1 Receptor Antagonist by Soluble IL-1 Receptors and levels of Soluble IL-1 Receptors in Synovial Fluids. *The Journal of Immunology* **1994**, 4766-4774.
5. Bienkowski, M. J.; Eessalu, T. E.; Berger, A. E.; Truesdell, S. E.; Shelly, J. A.; Laborde, A. L.; Zurcher-Neely, H. A.; Reardon, I. M.; Heinrikson, R. L.; Chosay, J. G.; et al., Purification and characterization of interleukin 1 receptor level antagonist proteins from THP-1 cells. *The Journal of biological chemistry* **1990**, *265* (24), 14505-11.
6. Takii, T.; Honda, H.; Sasayama, S.; Kobayashi, T.; Ikezawa, H.; Udaka, S.; Oomoto, Y.; Onozaki, K., Human interleukin-1 receptor antagonist: large-scale expression in *Bacillus brevis* 47-5Q. *J Interferon Cytokine Res* **1999**, *19* (11), 1325-31.
7. Dinarello, C. A., Biology of interleukin 1. *FASEB J* **1988**, *2* (2), 108-15.
8. Netea, M.; Nold-Petry, C. A.; Nold, M. F.; Joosten, L. A. B.; Opitz, B.; Meer, J. H. M. v. d.; Veerdonk, F. L. v. d.; Ferwerda, G.; Heinhuis, B.; Devesa, I.; Funk, C. J.; Mason, R. J.; Kullberg, B. J.; Rubartelli, A.; Meer, J. W. M. v. d.; Dinarello, C. A., Differential requirements for the activation of the inflammasome for processing and release of IL-1b in monocytes and macrophages. *Blood* **2009**, *113* (10), 2324-2335.
9. Thomas, C.; Bazan, J. F.; Garcia, K. C., Structure of the activating IL-1 receptor signaling complex. *Nat Struct Mol Biol* **2012**, *19* (4), 455-7.
10. Weber, A.; Wasiliew, P.; Kracht, M., Interleukin-1 (IL-1) pathway. *Sci Signal* **2010**, *3* (105), cm1.
11. Contassot, E.; Beer, H. D.; French, L. E., Interleukin-1, inflammasomes, autoinflammation and the skin. *Swiss medical weekly* **2012**, *142*, w13590.
12. Mancilla, J.; Ikejima, T.; Dinarello, C. a., Glycosylation of the Interleukin-1 Receptor Type I is Required for Optimal Binding of Interleukin-1. *Lymphokine and cytokine research* **1992**, *11* (4), 197-205.
13. Burger, D.; Dayer, J.-M., IL-1ra. *Cytokine Reference* **2000**.
14. Schreuder, H.; Tardif, C.; Trump-Kallmeyer, S.; Soffientini, A.; Sarubbi, E.; Akesson, A.; Bowlin, T.; Yanofsky, S.; Barrett, R. W., A new cytokine-receptor binding mode revealed by the crystal structure of the IL-1 receptor with an antagonist. *Nature* **1997**, *386* (6621), 194-200.
15. Fleischmann, R. M.; Schechtman, J.; Bennett, R.; Handel, M. L.; Burmester, G. R.; Tesser, J.; Modafferi, D.; Poulakos, J.; Sun, G., Anakinra, a recombinant human interleukin-1 receptor antagonist (r-metHuIL-1ra), in patients with rheumatoid arthritis: A large, international, multicenter, placebo-controlled trial. *Arthritis and rheumatism* **2003**, *48* (4), 927-34.
16. Aksentijevich, I.; Nowak, M.; Mallea, M.; Chae, J. J.; Watford, W. T.; Hofmann, S. R.; Stein, L.; Russo, R.; Goldsmith, D.; Dent, P.; Rosenberg, H. F.; Austin, F.; Remmers, E. F.; Balow, J. E., Jr.; Rosenzweig, S.; Komarow, H.; Shoham, N. G.; Wood, G.; Jones, J.; Mangra, N.; Carrero, H.; Adams, B. S.; Moore, T. L.; Schikler, K.; Hoffman, H.; Lovell, D. J.; Lipnick, R.; Barron, K.; O'Shea, J. J.; Kastner, D. L.; Goldbach-Mansky, R., De novo CIAS1 mutations, cytokine activation, and evidence for genetic heterogeneity in patients with neonatal-onset multisystem inflammatory disease (NOMID): a new member of the expanding family of pyrin-associated autoinflammatory diseases. *Arthritis and rheumatism* **2002**, *46* (12), 3340-8.
17. Cohen, S. B.; Moreland, L. W.; Cush, J. J.; Greenwald, M. W.; Block, S.; Shergy, W. J.; Hanrahan, P. S.; Kraishi, M. M.; Patel, A.; Sun, G.; Bear, M. B.; Study, G., A multicentre, double blind, randomised,

placebo controlled trial of anakinra (Kineret), a recombinant interleukin 1 receptor antagonist, in patients with rheumatoid arthritis treated with background methotrexate. *Ann Rheum Dis* **2004**, *63* (9), 1062-8.

18. Team, M. G. C. P.; Temple, G.; Gerhard, D. S.; Rasooly, R.; Feingold, E. A.; Good, P. J.; Robinson, C.; Mandich, A.; Derge, J. G.; Lewis, J.; Shoaf, D.; Collins, F. S.; Jang, W.; Wagner, L.; Shenmen, C. M.; Misquitta, L.; Schaefer, C. F.; Buetow, K. H.; Bonner, T. I.; Yankie, L.; Ward, M.; Phan, L.; Astashyn, A.; Brown, G.; Farrell, C.; Hart, J.; Landrum, M.; Maidak, B. L.; Murphy, M.; Murphy, T.; Rajput, B.; Riddick, L.; Webb, D.; Weber, J.; Wu, W.; Pruitt, K. D.; Maglott, D.; Siepel, A.; Brejova, B.; Diekhans, M.; Harte, R.; Baertsch, R.; Kent, J.; Haussler, D.; Brent, M.; Langton, L.; Comstock, C. L.; Stevens, M.; Wei, C.; van Baren, M. J.; Salehi-Ashtiani, K.; Murray, R. R.; Ghamsari, L.; Mello, E.; Lin, C.; Pennacchio, C.; Schreiber, K.; Shapiro, N.; Marsh, A.; Pardes, E.; Moore, T.; Lebeau, A.; Muratet, M.; Simmons, B.; Kloske, D.; Sieja, S.; Hudson, J.; Sethupathy, P.; Brownstein, M.; Bhat, N.; Lazar, J.; Jacob, H.; Gruber, C. E.; Smith, M. R.; McPherson, J.; Garcia, A. M.; Gunaratne, P. H.; Wu, J.; Muzny, D.; Gibbs, R. A.; Young, A. C.; Bouffard, G. G.; Blakesley, R. W.; Mullikin, J.; Green, E. D.; Dickson, M. C.; Rodriguez, A. C.; Grimwood, J.; Schmutz, J.; Myers, R. M.; Hirst, M.; Zeng, T.; Tse, K.; Mokska, M.; Deng, M.; Ma, K.; Mah, D.; Pang, J.; Taylor, G.; Chuah, E.; Deng, A.; Fichter, K.; Go, A.; Lee, S.; Wang, J.; Griffith, M.; Morin, R.; Moore, R. A.; Mayo, M.; Munro, S.; Wagner, S.; Jones, S. J.; Holt, R. A.; Marra, M. A.; Lu, S.; Yang, S.; Hartigan, J.; Graf, M.; Wagner, R.; Letovksy, S.; Pulido, J. C.; Robison, K.; Esposito, D.; Hartley, J.; Wall, V. E.; Hopkins, R. F.; Ohara, O.; Wiemann, S., The completion of the Mammalian Gene Collection (MGC). *Genome Res* **2009**, *19* (12), 2324-33.
19. Wu, S.; Letchworth, G. J., High efficiency transformation by electroporation of *Pichia pastoris* pretreated with lithium acetate and dithiothreitol. *Biotechniques* **2004**, *36* (1), 152-4.
20. Page, C. N.; Vajdos, F.; Fee, L.; Grimsley, G.; Gray, T., How to measure and predict the molar absorption coefficient of a protein. *Protein Science* **1995**, *4*, 2311-2423.
21. Hamilton, B. S.; Brede, Y.; Tolbert, T. J., Expression and characterization of human glycosylated interleukin-1 receptor antagonist in *Pichia pastoris*. *Protein Expr Purif* **2008**, *59* (1), 64-8.
22. Guimaraes, C. P.; Witte, M. D.; Theile, C. S.; Bozkurt, G.; Kundrat, L.; Blow, A. E. M.; Ploegh, H. L., Site-specific C-terminal and internal loop labeling of proteins using sortase-mediated reactions. *Nature Protocols* **2013**, *8* (9), 1787-1799.
23. Amine-Reactive Probes. In *Life Technologies, Probes*, M., Ed. 2013; Vol. MAN0001774.
24. Daly, R.; Hearn, M. T., Expression of heterologous proteins in *Pichia pastoris*: a useful experimental tool in protein engineering and production. *Journal of molecular recognition* **2005**, *18* (2), 119-138.
25. Tsukiji, S.; Nagamune, T., Sortase-Mediated Ligation: A Gift from Gram-Positive Bacteria to Protein Engineering. *ChemBioChem* **2009**, *10* (5), 787-798.
26. Instant Determination of Protein Presence Using the BLItz System. In *forteBio, Sciences*, P. L., Ed. 2013; Vol. Application note 4.
27. Hulme, E. C.; Trevethick, M. A., Ligand binding assays at equilibrium: validation and interpretation. *British Journal of Pharmacology* **2010**, *161*, 1219-1237.

Appendices

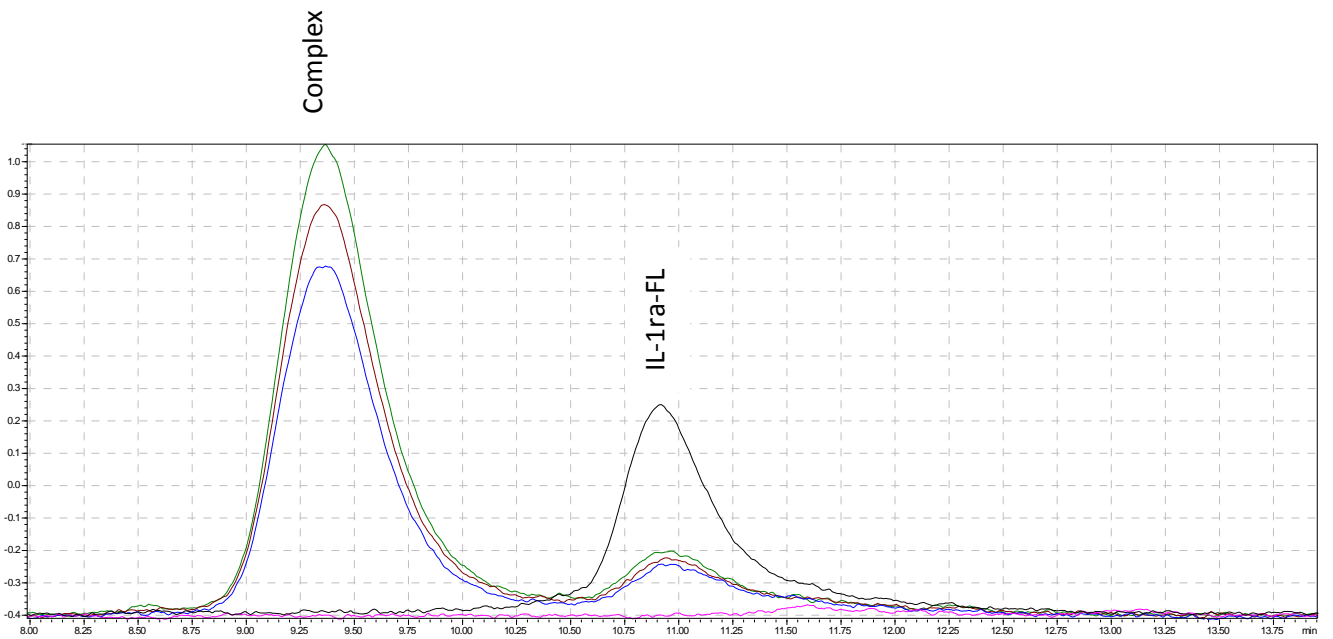


Figure A1. 5000 pM IL-1R1 + 500 pM IL-1ra-FL. Black: IL-1ra-FL, Green: Complex run 1, Brown: Complex run 2, Blue: Complex run 3, Pink: Baseline.

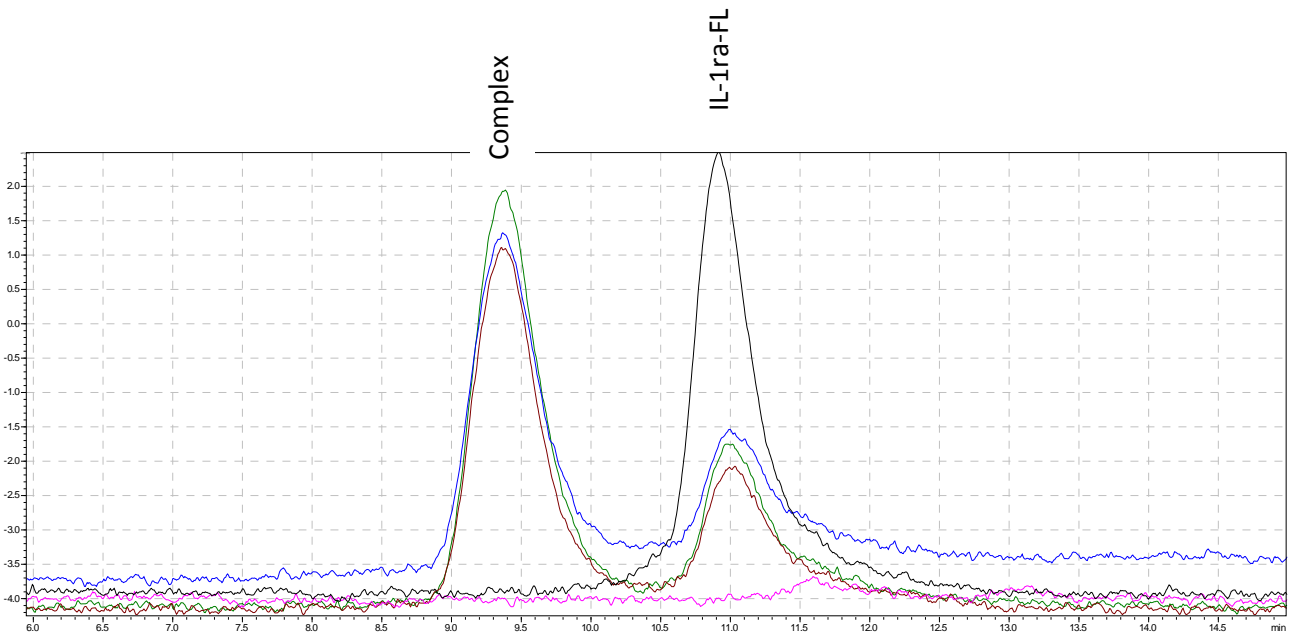


Figure A2. 2500 pM IL-1R1 + 500 pM IL-1ra-FL. Black: IL-1ra-FL, Green: Complex run 1, Brown: Complex run 2, Blue: Complex run 3, Pink: Baseline.

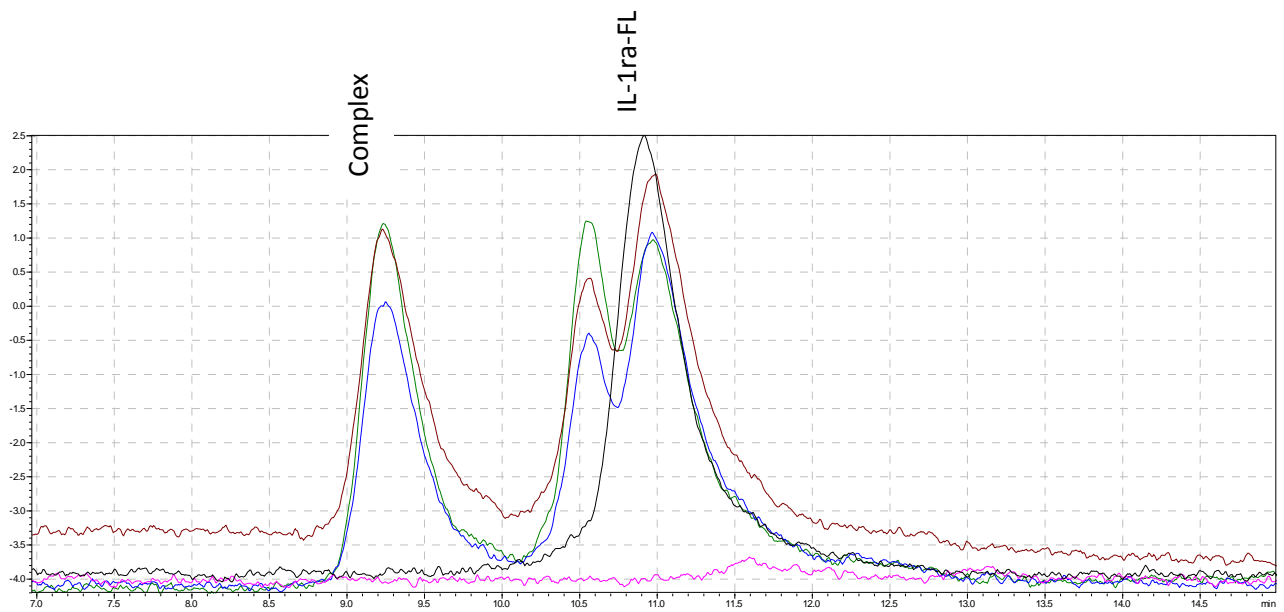


Figure A3. 1250 pM IL-1R1 + 500 pM IL-1ra-FL. Black: IL-1ra-FL, Green: Complex run 1, Brown: Complex run 2, Blue: Complex run 3, Pink: Baseline.

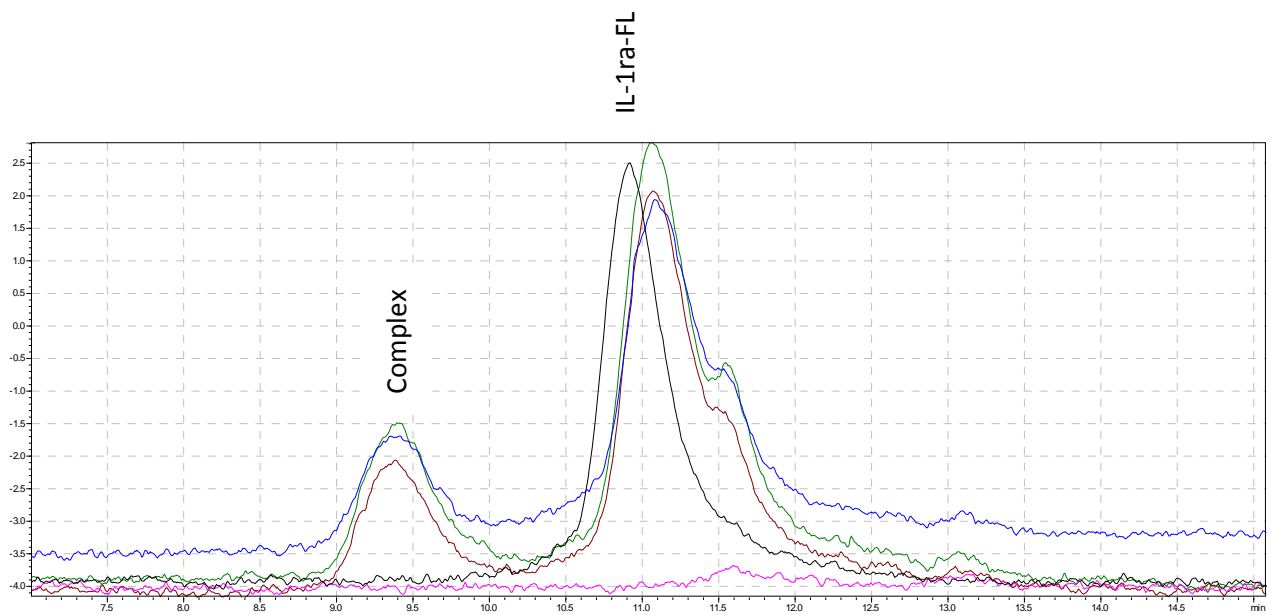


Figure A4. 625 pM IL-1R1 + 500 pM IL-1ra-FL. Black: IL-1ra-FL, Green: Complex run 1, Brown: Complex run 2, Blue: Complex run 3, Pink: Baseline.

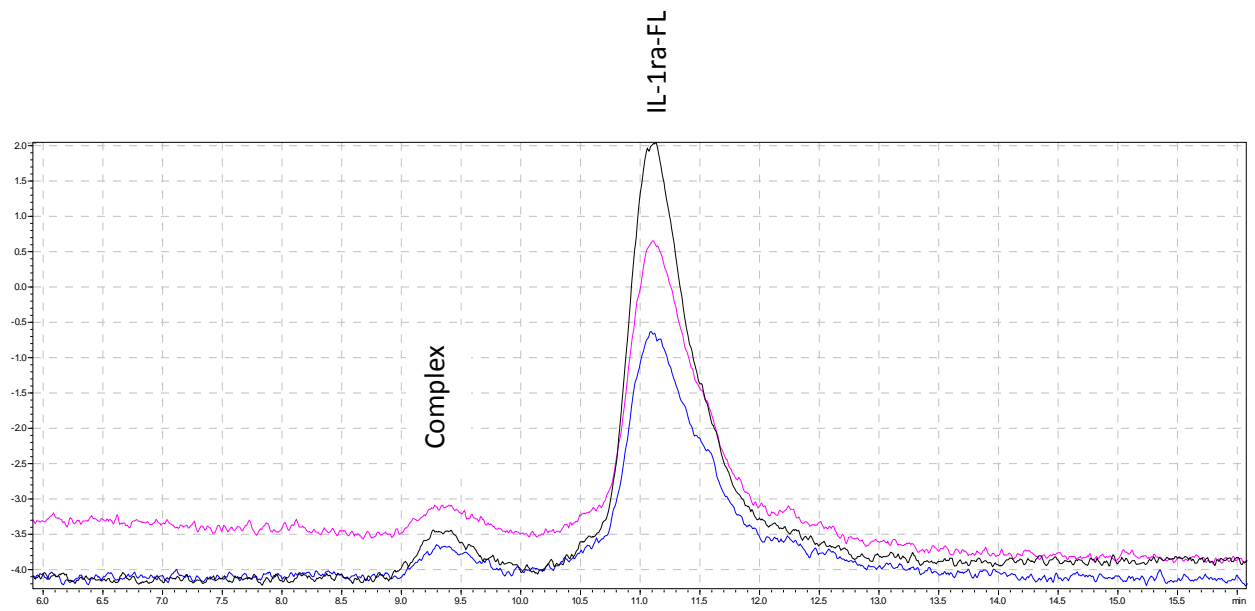


Figure A5. 312 pM IL-1R1 + 500 pM IL-1ra-FL. Black: Complex run 1, Pink: Complex run 2, Blue: Complex run 3.

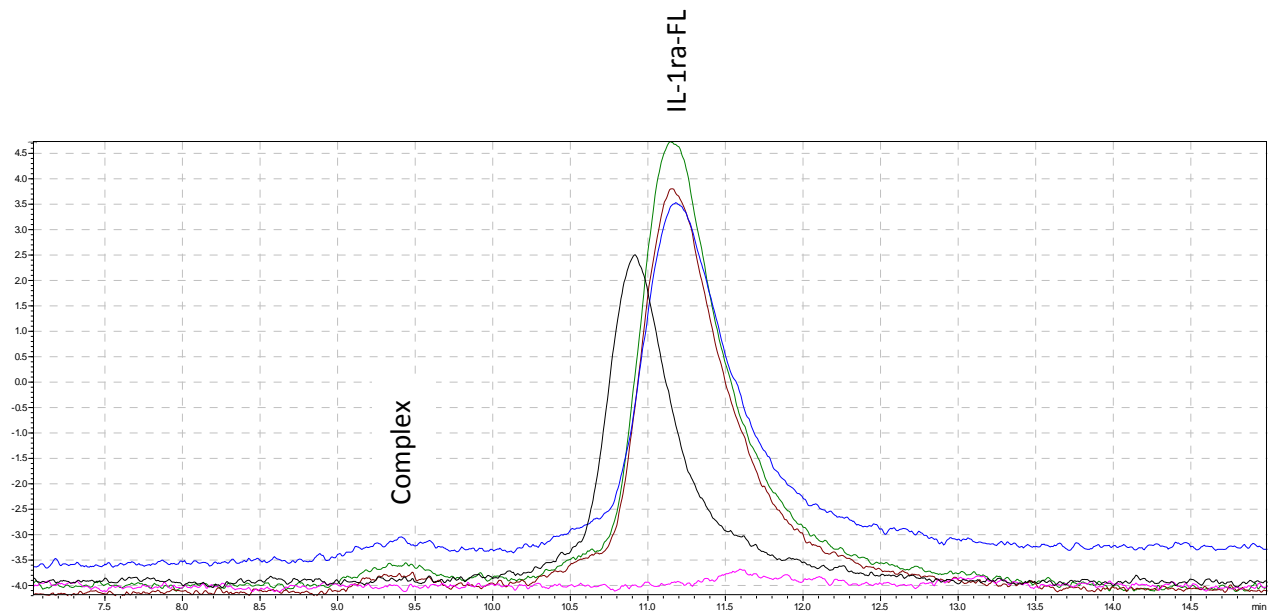


Figure A6. 156 pM IL-1R1 + 500 pM IL-1ra-FL. Black: IL-1ra-FL, Green: Complex run 1, Brown: Complex run 2, Blue: Complex run 3, Pink: Baseline.

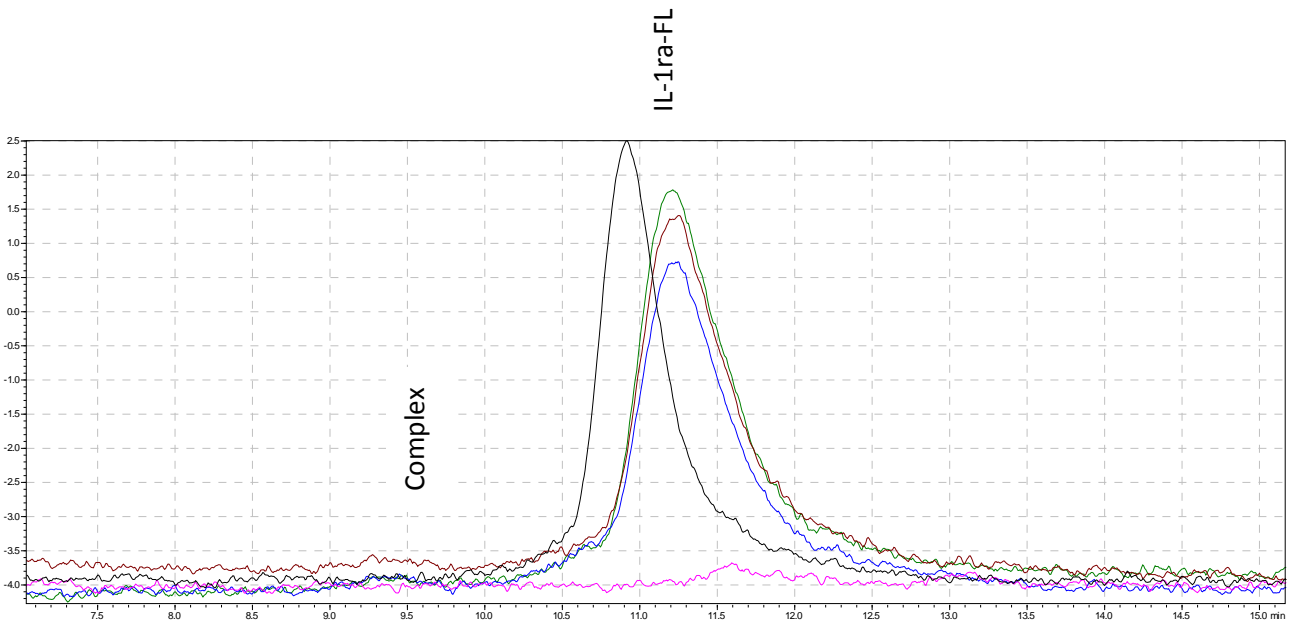


Figure A7: 75 pM IL-1R1 + 500 pM IL-1ra-FL. Black: IL-1ra-FL, Green: Complex run 1, Brown: Complex run 2, Blue: Complex run 3, Pink: Baseline.